THE ROLE OF THE *STAPHYLOCOCCUS LUGDUNENSIS* ISD SYSTEM IN IRON
ACQUISITION AND BIOFILM FORMATION

By

Kathryn Patricia Haley

Dissertation

Submitted to the Faculty of the

Graduate School of Vanderbilt University

in partial fulfillment of the requirements

for the degree of

DOCTOR OF PHILOSOPHY

In

Microbiology and Immunology

August 2014

Nashville, Tennessee

Approved:

Andrew Link, Ph.D.

Timothy L. Cover, M.D.

Seth R. Bordenstein, Ph.D.

Richard M. Peek, M.D.

Eric P. Skaar, Ph.D.

TABLE OF CONTENTS

Acknowledgements

Lastly, I would like to thank my family. You have been a constant source of support. You believed in my when I doubted myself and gave me the courage to dream big. I would also like to give a special thanks to my amazing husband, Eric Janson. I cannot imagine navigating graduate school without your love, support and humor.

"and it was the best two weeks of our lives…" Eric Janson

LIST OF FIGURES

LIST OF ABBREVIATIONS

CFU   colony forming units

CNS   coagulase-negative Staphylococcus

Dip   2, 2-dipyridyl

Isd   iron-regulated surface determinant system

Fur   ferric uptake regulator

Glc-*NA*c   *N*-acetylglucosamine

HPLC   high pressure liquid chromatography

HRESIMS   high resolution electrospray ionization mass spectrometry

MuDPIT   multi-dimenstional protein identification technology

Mur*NA*c   *N*-acetylmuramic acid

PBS   phosphate-buffered saline

PG   peptidoglycan

PMSF   phenylmethylsulphonyl fluoride

SDS   sodium dodecyl sulfate

TBS   tryptic soy broth

vWbp   von Willebrand binding factor protein

Chapter I

INTRODUCTION

Staphylococcus lugdunensis

S. lugdunensis is a coagulase negative Staphylococcus (CNS) that is often found as part of the normal skin flora and has the potential to cause aggressive infections similar to those caused by *S. aureus*. *S. lugdunensis* is emerging as an important human pathogen with characteristics that make it stand out from other CNS, including its increased level of virulence [1, 2]. Unlike other CNS, *S. lugdunensis* has the capacity to cause a wide array of serious infections such as acute endocarditis, brain abscesses, meningitis, prosthetic joint infections, pneumonia, toxic shock and necrotizing fasciitis [3, 4]. The mortality rate associated with *S. lugdunensis* endocarditis can reach 50% [5] which presents a serious public health problem considering the propensity of *S. lugdunensis* to infect the heart. This is in striking contrast to the 14.5% mortality rate associated with *S. aureus* endocarditis, and the 20% mortality rate associated with *Staphylococcus epidermidis* endocarditis [5]. The ability of *S. lugdunensis* to cause necrotizing fasciitis has only recently been documented and exemplifies an alarming trend for pathogenic bacteria to develop greater degrees of virulence. Additionally, the majority of infections caused by S. *lugdunensis* occur in healthy adults, primarily in the outpatient setting [6]. In fact, nearly half of patients infected with *S. lugdunensis* do not exhibit identifiable comorbidities. This indicates that *S. lugdunensis* is not confined to being an opportunistic pathogen, another fact which distinguishes it from other CNS [6]. Although *S. lugdunensis* remains highly susceptible to the majority of antimicrobial therapies, antibiotic resistance is evolving [6]. The number of *S. lugdunensis* isolates that are

susceptible to all antibiotics has decreased from 68% in 1993 to 45% in 2010 [6, 7]. Additionally, the prevalence of ampicillin resistant strains is increasing, and *mecA* positive *S. lugdunensis* isolates has been identified [6, 8]. This increase in antibacterial resistance coupled with the substantial virulence of this organism presents a clinical challenge that necessitates a more thorough understanding of the molecular determinants of virulence within *S. lugdunensis*.

Many of the infections associated with *S. lugdunensis* (native valve endocarditis, prosthetic joint infection and intravascular catheter infection) are linked to biofilm formation [9, 10]. Few virulence factors have been identified within *S. lugdunensis* however those that have been described give insight into how this pathogen is able to adhere to host tissues and proliferate. For example, *S. lugdunensis* encodes fibrinogen binding protein, Fbl which is closely related to Clumping Factor A, Clf, from *S. aureus*. Importantly, Clf has been shown to be involved in adherence in an endocarditis model of *S. aureus* infection [11, 12]. Additionally, *S. lugdunensis* expresses a von Willebrand binding factor protein (vWbp) which aids in the establishment of infectious legions within *S. aureus* [13]. While *S. lugdunensis* does not encode an alpha hemolysin as does *S. aureus,* it does encode a delta hemolysin, enabling access to host hemoglobin [14]. This delta hemolysin in coordination with the *S. lugdunensis* Iron-regulated surface determinant (Isd) system is predicted to allow for nutrient iron acquisition during infection. Included in the *S. lugdunensis* Isd system is an IsdG-family heme oxygenase as well as the predicted peptidoglycan (PG) hydrolase, PghI. The role and regulation of both IsdG and PghI is discussed in detail within Chapters II and III.

Peptidoglycan Hydrolases

The PG cell wall is an essential feature of the Gram-positive cell and protects the cellular membrane from osmotic rupture. PG is composed of polysaccharide strands that are covalently linked by crosslinking peptide moieties forming a continuous molecule that encases the cell [15]. Since bacteria are sheathed in this polymeric shell, bacterial growth and division are inherently linked to the synthesis and destruction of the PG layer. To prevent a critical loss of cellular resources, many bacteria recycle up to half of their cell wall per generation [16]. While PG hydrolysis is critical for bacterial growth, uncontrolled degradation of the cell wall will lead to lysis. Consequently, the expression of PG hydrolases is highly regulated. Since PG synthesis is critical for bacterial division and survival and PG is structurally unique to bacteria many antibiotics target the enzymes involved in PG synthesis [16].

PG hydrolases are a large and diverse group of enzymes capable of cleaving polymeric bonds within both the PG saculli and soluble PG fragments [17]. Assigning a specific function to any one hydrolase is challenging because most bacteria encode numerous hydrolases often with redundant functions. Additionally, many hydrolases perform multiple functions and can recognize and cleave PG at various bonds. In fact, for every amide and glycosidic bond within the PG structure, a hydrolase enzyme which can cleave it has been identified [17]. Additionally, hydrolases are often specific for a certain type of PG and can even be species specific. PG hydrolases can be grouped based on where in the PG molecule they cleave. Muramidases including lysozymes and lytic transglycosylases cleave the glycosidic bonds between *N*-acetylmuramic acid (Mur*NA*c)

and *N*-acetylglucosamine (Glc*NA*c) while *N*-acetylmuramyl-ʟ-alanine amidases hydrolyse the amide bond between Mur*NA*c and ʟ-alanine whereas carboxy and endopeptidases cleave the bonds between various stem peptides [17].

While PG hydrolases are involved in basic cellular functions, they have also been shown to play a critical role during pathogenesis. The autolysin LytF$_{sm}$ is up-regulated in *Streptococcus mutans* in response to cellular stress and subsequent activation of the SigX regulon by the quorum sensing peptide, competent-stimulating peptide (CSP). Expression of LytF$_{sm}$ causes lysis of a portion of cells, resulting in the production of extracellular DNA (eDNA) and increased survival of the remaining cells. This increased survival is likely due to the uptake of the released DNA [18]. PG is a potent immune activator and the release of PG subunits by hydrolases within *Listeria monocytogenes* modulate the innate immune response through natural killer (NK) cell activation and contribute to pathogenicity [19]. Additionally, the enzymatic activity of the PG hydrolase LytC within *Streptococcus pneumonia* diverts the deposition of C3b on the surface of bacteria and consequently mitigates the effect of complement-mediated immunity [20]. Lastly, both the PG modifying activities and lytic capabilities of PG hydrolases promote bacterial adherence and biofilm formation. Recurrent and persistent bacterial infections are frequently observed in patients with indwelling medical devices. The pathogenesis of these infections is dependent upon the ability of bacteria to first adhere to the device and then generate a biofilm. These biofilms are complex communities of bacteria that are encased within a matrix and display distinct phenotypes. Staphylococcal cells embedded within this matrix are inherently resistant to both the host immune system as well as antimicrobial therapies [21]. Furthermore, biofilms can complicate infections by serving

as a focus of infection from which bacteria can disseminate resulting in bloodstream infection, emboli, and metastatic infections [21]. The autolytic activity of some PG hydrolases generates eDNA which assists bacterial adherence to surfaces as well as neighboring bacteria [22]. The major autolysin within *S. epidermidis*, AtlE, is localized to the cell surface and is involved in the primary attachment of cells to polystyrene surfaces [23]. Importantly, homologs of AtlE have been identified in multiple staphylococcal species including *S. aureus* and *S. lugdunensis*. I have found that *S. lugdunensis* encodes an additional PG hydrolase, *pghl,* which promotes biofilm formation and is unique among PG hydrolases in that it is iron-regulated. This type of transcriptional regulation suggests *pghl* is expressed during infection and is therefore likely to play a role in pathogenesis. The enzymatic characterization and transcriptional regulation of *pghl* is described in Chapter III.

Iron and Infection

A promising strategy to combat bacterial infections is to inhibit the procurement of nutrients that are necessary for growth. Iron is required by nearly all living organisms and *S. lugdunensis* is no exception. In a process referred to as nutritional immunity, the vertebrate host tightly regulates iron levels and sequesters this valuable nutrient intracellularly as a mechanism to prevent bacterial proliferation.

Host iron sequestration is a complex process requiring the synchronization of multiple enzymes involved in host iron regulation. Iron is insoluble at physiologic pH found within vertebrate tissues and any free iron is quickly removed by high-affinity iron binding proteins. Within the serum, free iron is bound by transferrin with an association constant

of approximately 10^{36} (Figure 1) [24]. In addition to binding free iron, transferrin functions as an iron transport protein, transferring iron to peripheral tissues through receptor-mediated endocytosis of transferrin receptor 1 (TfR1) [25]. Iron levels are also limited in lymph and mucosal secretions through lactoferrin, which quickly binds all free iron. Additionally, lactoferrin is a major component within phagocytes, ensuring that engulfed pathogens have limited access to intracellular iron. In healthy individuals both lactoferrin and transferrin are only 30-40% saturated and consequently are poised to bind free iron [24].

The overwhelming majority of iron within humans is found in the form of heme; a tetrapyrrole ring with a coordinated iron center. Heme is often bound by hemoproteins, the most abundant of which is hemoglobin. To further prevent access to iron, hemoglobin is sequestered intracellularly within erythrocytes; greater than 90% of iron within the human body is located intracellularly making it inaccessible to extracellular pathogens unless mechanisms are employed to liberate these rich sources of nutrient iron (Figure 1) [26]. Although hemoglobin is the most abundant hemoprotein in the body, there are additional heme-binding proteins that can serve as sources of iron for invading bacteria. Haptoglobin is a tetrachain (α2β2) glycoprotein that binds free hemoglobin (Figure 1) following hemolysis as a means to prevent loss of iron through urinary excretion and subsequent kidney damage [27]. *S. aureus* binds haptoglobin-hemoglobin complexes *in vitro,* suggesting that this protein complex is exploited as a source of nutrient iron [28]. While it remains unknown if *S. lugdunensis* can bind haptoglobin-hemoglobin, the high degree of homology between the iron acquisition systems of *S. aureus* and *S. lugdunensis* makes it reasonable to speculate that *S. lugdunensis* binds haptoglobin.

Myoglobin is an additional hemoprotein that is found within myocytes. *S. aureus* can utilize myoglobin as an iron source *in vitro* and this protein may represent a source of iron during colonization of muscle tissue [29]. While it is unclear if *S. aureus* or *S. lugdunensis* utilize myoglobin during infection, it is likely that the tissue damage that occurs during skin and soft tissue infections would provide these bacteria with significant access to this rich heme-iron source. In support of this contention, both *S. lugdunensis* and *S. aureus* readily colonizes the heart and damage surrounding cardiac myocytes [30].

Nutritional immunity is a dynamic process that is capable of responding to assaults from invading bacteria. A primary coordinator of this response is the hepatic peptide hormone hepcidin, which regulates iron absorption and the distribution of iron within tissues. All iron within the body, whether it is dietary iron entering through duodenal enterocytes, or iron within macrophages that have recycled senescent erythrocytes, must leave the cells to enter circulating plasma. Inflammation is one of the many stimulatory signals that affect hepcidin concentrations within the serum. Specifically, induction of IL-6 production and LPS-mediated TLR4 signaling both cause increases in circulating hepcidin [31]. Inflammation-induced increases in hepcidin represent a hypoferremic response to infection, which allows the host to respond to bacterial assault by further reducing available iron and preventing bacterial replication [31]. Together hepcidin, transferrin, and lactoferrin function to maintain an extracellular environment free of elemental iron. In summary, iron homeostasis within the human host requires the integration of multiple signals, resulting in an environment that is iron-deplete and able to respond to bacterial assault.

Iron and Infection

1. Staphylococcal hemolysins lyse open erythrocytes.

2. Hemoglobin is released into the extracellular milieu following erythrocyte lysis.

3. Haptoglobin binds free hemoglobin preventing heme loss.

4. Free heme can be acquired by *S. lugdunensis* through the Isd system and HtsBC system in *S. aureus.*

5. Free hemoglobin can be used as an iron source by *S. lugdunensis* using Isd proteins.

6. Siderophores remove iron from transferrin to be used as an iron source.

Transferrin Hemoglobin

Haptoglobin

Staphyloferrin A

Hemolysin

heme

Iron

Figure 1.

Model depicting both host factors involved in nutritional immunity as well as bacterial factors utilized to circumvent host sequestration of iron.

Heme Oxygenases

Heme oxygenases are a ubiquitous family of enzymes which catabolize heme. All identified heme oxygenases can be categorized into one of two families, the HO-1 family that is conserved across kingdoms and the IsdG family that has only been identified in Bacteria. HO-1 family heme oxygenases degrade heme to the blue-green molecule biliverdin with the concomitant production of carbon monoxide. In vertebrates biliverdin is further reduced to bilirubin by biliverdin reductase. In contrast, IsdG and IsdI degrade heme to staphylobilin, a yellow oxo-bilirubin molecule, and formaldehyde [32] with the exception of the *M. tuberculosis* IsdG which degrades heme to mycobilin [33]. Both bilirubin and biliverdin have potent antioxidant properties within humans however; the role of heme degradation products within bacteria has not been elucidated. The importance of both bilirubin and biliverdin to human physiology makes it tempting to speculate that staphylobilin may serve important biological functions within bacteria. Furthermore, carbon monoxide produced during HO-1 mediated heme catabolism serves as a signaling molecule within humans. Considering the conservation of IsdG family members across numerous bacterial pathogens, identifying the function of staphylobilin as well as formaldehyde may have broad implications to numerous infectious diseases.

S. aureus encodes two seemingly redundant heme oxygenases, IsdG and IsdI. While both enzymes bind and degrade heme, they are differentially regulated indicating a possible rationale for encoding two paralogous heme oxygenases [34, 35]. Both *isdG* and *isdI* transcript levels increase in iron-deplete conditions and are subjected to Fur-mediated regulation [34]. IsdG however, undergoes proteolytic degradation in the absence of the substrate heme [34]. This suggests that *S. aureus* differentially regulates

IsdG and IsdI to precisely adjust the level of heme catabolism within the cell in response to alterations in cellular heme concentrations [34]. *S. lugdunensis* also expresses IsdG which is 68% identical to *S. aureus* IsdG at the amino acid level however I found that *S. lugdunensis* IsdG is stable in the absence of heme. This indicates that structural differences exist within *S. lugdunensis* IsdG that prevent it from being targeted for degradation. Alternatively, *S. lugdunensis* may not encode the protease responsible for the targeted degradation of *S. aureus* IsdG. The role and regulation *of S. lugdunensis* IsdG is described in detail in Chapter II.

The *S. lugdunensis* Isd system

While the vertebrate host has evolved sophisticated mechanisms by which it sequesters iron from invading pathogens, *S. lugdunensis* has evolved equally sophisticated mechanisms to gain access to iron during infection. For example, Fur-mediated regulation allows *S. lugdunensis* to respond to iron starvation through the dramatic up-regulation of Isd system [36]. The Isd system includes the cell wall anchored heme binding proteins (IsdC, IsdJ, and IsdK), a wall anchored hemoglobin receptor (IsdB), a membrane transporter (IsdEF), and a cytoplasmic heme oxygenase (IsdG) [36-38]. The Isd system also includes sortase B, an enzyme dedicated to anchoring IsdC to the cell wall and is also predicted to anchor IsdK to the cell wall. Conversely, IsdB and IsdJ are predicted to be anchored to the cell wall by sortase A [38, 39]. These proteins are hypothesized to work in concert to enable *S. lugdunensis* to utilize vertebrate hemoglobin as a source of nutrient iron.

IsdB, IsdC, IsdJ and IsdK contain NEAr iron Transporter (NEAT) domains [36]. NEAT domains are conserved stretches of amino acids that mediate heme and hemoprotein binding [40]. Heme-iron is bound within these clefts by a single axial tyrosine ligand [41]. The current model for heme acquisition via the *S. lugdunensis* Isd system proposes that IsdB employs NEAT domains to initiate the process by binding hemoglobin. IsdB then transfers heme to IsdC which transfers the porphyrin through the cell wall. It is then predicted that heme is transferred to IsdEF which passes heme through the cell membrane into the cytoplasm where it is degraded by IsdG. Interestingly, while both IsdJ and IsdK are predicted to be linked to the cell wall based on the presence of sortase A and sortase B signals respectively; a recent study found that the majority of IsdJ and IsdK are localized to the membrane [36]. Furthermore, the role of both IsdJ and IsdK in iron acquisition remains unclear. The Isd system represents a paradigm of heme-iron acquisition, and illustrates a mechanism by which bacterial pathogens utilize hemoglobin as an iron source and traffic heme inside the cell.

To achieve an extracellular environment virtually free of iron vertebrate hosts produce the iron-sequestering proteins transferrin and lactoferrin. To combat this sequestration *S. aureus* elaborates siderophores, small molecules with an impressively high affinity for iron which target and remove iron bound to transferrin and lactoferrin (Figure 1). These siderophores are conserved within the *S. lugdunensis* genome however; it has not been conclusively shown that the protein products of these genes function as siderophores. Production of siderophores in *S. aureus* is Fur-regulated and consequently increases when the bacteria experience iron stress [42, 43]. Bacterial siderophores can be synthesized using two distinct pathways, the non-ribosomal peptide synthetases (NRPS)

pathway and the NRPS-independent (NIS) pathway. The NRPS pathway synthesizes siderophores using modular enzymatic platforms [44]. In contrast, the NIS pathway utilizes condensation reactions with units of dicarboxylic acids, diamines and amine alcohols to create the final siderophore structure [44]. *S. aureus* encodes for two siderophores, staphyloferrin A and staphyloferrin B, and both are synthesized through the NIS pathway and then secreted into the extracellular milieu. Within *S. aureus* both staphyloferrin A and staphyloferrin B, upon binding iron, are transported into the cytoplasm through the ABC transporters HtsABC and the *s*taphylococcal *i*ron *r*egulated transporter (SirABC), respectively [44]. Additionally, HtsBC has been found to transport heme into the cytoplasm suggesting that HtsABC may serve as a dual iron/heme transporter [45]. Siderophore production in combination with the Isd system provides *S. aureus* and presumably *S. lugdunensis* multiple routes for obtaining iron.

Chapter II

***STAPHYLOCOCCUS LUGDUNENSIS* ISDG LIBERATES IRON FROM HOST HEME**

Introduction

Iron acquisition is a critical process for pathogenic bacteria during infection. This is due to the numerous fundamental cellular processes that require iron such as DNA replication, electron transport and protection from reactive oxygen damage [46]. Vertebrates exploit the iron requirement of bacterial pathogens by creating an extracellular environment virtually devoid of free iron. The most abundant source of iron within the human body is found in the form of heme, a tetrapyrole ring with a coordinated iron center. Heme is further bound by hemoproteins the most abundant of which is hemoglobin. To circumvent this sequestration, pathogenic bacteria have evolved complex iron acquisition systems that they elaborate upon entry into host tissues. In Gram-positive bacteria one such system is the Isd system which binds hemoglobin, removes the heme cofactor, and transports heme inside the bacterial cytoplasm where it is degraded by heme oxygenases resulting in the release of nutrient iron [32, 47]. Interestingly, heme is the preferred source of iron for *S. aureus* during infection [45], and heme acquisition by the Isd system is critical for full virulence in *S. aureus* [34].

The sequencing of the *S. lugdunensis* genome has allowed for a more in depth analysis of the genes underlying the virulence of this dynamic pathogen [48]. In this regard, *S. lugdunensis* encodes a complete Isd system including an IsdG heme oxygenase. This observation suggests that *S. lugdunensis* is capable of using heme as a source of iron

during infection. Here I use biochemical and genomic techniques to characterize this member of the IsdG family of heme degrading oxygenases and provide insight into the nutrient acquisition pathways of *S. lugdunensis*.

Methods

Protein purification

Recombinant *S. lugdunensis* IsdG was purified from *Escherichia coli* BL21 (DE3) carrying the pET-15b-*isdG* plasmid. Overnight cultures were grown at 37° in TSB with 100 µg/ml ampicillin and 34 µg/ml chloramphenicol. The next day cells were diluted in fresh media and grown to mid-log phase at which time expression was induced through the addition of 1mM isopropyl-1-thiol-(D)-galactopyranoside. Cell growth continued for 3 H at 30° after which time cells were collected through centrifugation at 8,000 x *g* for 10 min. Cell pellets were then washed with 50 mM Tris-HCl (pH 7.5) 100 mM NaCl, collected through centrifugation and stored at -80°. To collect recombinant protein cells were thawed on ice and resuspended in 50 mM Tris-HCl (pH 7.5) 100 mM NaCl with 100 µM phenylmethylsulfonyl fluoride. Cells were lysed using a French press and the cell suspension was centrifuged at 100,000 x *g* for 60 min. After centrifugation the soluable fraction was filter through a 0.45 µm filter and then applied to a Ni-Nitrilotriacetic acid column that had been pre-equilibrated with 50 mM Tris-HCl (pH 7.5), 100 mM NaCl. The column was then washed with two volumes of 50 mM Tris-HCl (pH 7.5) 100 mM NaCl followed by a wash using three volumes of 50 mM Tris-HCl (pH 7.5), 100 mM NaCl with 10% glycerol and 10 mM imidazole. Protein was eluted with 50 mM Tris-HCl (pH 7.5), 100 mM NaCl containing 500 mM imidazole. Proteins were then dialyzed against 50 mM Tris-HCl (pH 7.5), 100 mM NaCl. Protein concentrations were determined using a BCA assay and purity was evaluated by SDS-PAGE.

Heme degradation and product purification

Heme degradation reactions were performed in 50 mM tris, pH 7.5, 150 mM NaCl at room temperature. Forty µM purified IsdG or mutant IsdG was incubated with 40 µM hemin (Sigma) for 30 minutes at 4° to allow heme protein complexes to form. Catalase (from bovine liver, Sigma) was added to the sample at a 0.5:1 molar ratio of catalase: hemoprotein, ascorbic acid was added to a final concentration of 1 mM and spectral changes between 300 and 800 nm were measured at 15, 30, 60, and 90 min after the addition of ascorbate. Purification of heme degradation products were done as before [32].

HPLC analysis was performed on a Varian ProStar using a Microsorb-MV C-18 column. Analysis was performed with a flow rate of 1 ml min^{-1} using 95% water/5% acetonitrile with 0.1% TFA as the mobile phase. The mobile phase increased linearly from 5% to 80% over a 45 min time period. Staphylobilin peaks eluted at approximately 32 min or 60% mobile phase.

Difference absorption spectroscopy

All absorption spectra were obtained using a Varian Cary 50BIO. Heme binding analyses were performed using difference absorption spectroscopy at 413 nm. Aliquots of hemin (2 µM-28 µM) were added to both a sample aliquot (10 µM IsdG) and a reference aliquot of tris-buffered saline (50 mM tris, pH 7.5, 150 mM NaCl). Samples were incubated at 4° on a rotisserie for 30 min to allow ample time for protein heme complexes to form.

Heme binding assay

The Soret band of a 10 µM sample of purified IsdG was measured as hemin was added incrementally. The heme concentrations measured ranged from 2 µM-40 µM. After each addition of heme the sample was incubated at 4° on a rotisserie to allow time for heme protein complexes to form.

Heme utilization assay

To assess the ability of *S. lugdunensis* IsdG to degrade heme and allow for its use as an iron source a liquid growth assay was utilized. The clinical *S. aureus* isolate strain Newman was used in all experiments [49]. All strains were transformed with the p*OS1plgt* vector [50, 51]. For phenotypic complementation experiments, strains were created by transforming *S. aureus ΔisdGΔisdI* with the p*OS1*-derived vector containing a full length copy of *S. lugdunensis isdG* under the control of the *S. aureus* lipoprotein diacylglycerol transferase (*lgt*) constitutive promoter. Strains were grown overnight in RPMI with 10% casamino acids, the appropriate antibiotic and 0.5 mM EDDHA. Cultures were normalized to an OD_{600} of 0.6 and subcultured 1:100 into NRPMI with 100 µM $CaCl_2$, 25 µM $ZnCl_2$, 1 mM $MgCl_2$, 25 µM $MnCl_2$, 1 µM heme and the appropriate antibiotic. OD_{600} was measured over 55 H. The assay was repeated to test three biological replicates in triplicate.

Quantitative immunoblot

Cultures were grown overnight in TSB or TSB with 100-350 µM 2,2'-dipyridyl (Dip). Protoplasts were prepped and total protein concentrations normalized using a BCA assay. Samples were run analyzed using a 15% SDS-PAGE and then transferred to a nitrocellulose membrane. Membranes were stained with α-IsdG polyclonal antibody and

then stained with goat anti-rabbit conjugated antibody. Membranes were imaged using an Odyssey infrared imager. To analyze the effect of heme on cytoplasmic IsdG levels cultures were grown overnight in TSB with 350 µM Dip and increasing concentrations of heme. Samples were prepped and stained as previously described.

IsdG-family phylogenetic tree

We reconstructed the evolutionary relationships of IsdG/I using amino acid sequences obtained from bacterial species with annotated IsdG family heme oxygenases. We looked for IsdG proteins in NCBI GenBank using a tBLASTx search of the nr nucleotide database restricted to bacteria. *Staphylococcus aureus*, *Bacillus anthracis*, *Mycobacterium tuberculosis*, and *Bradyrhizobium japonicum* isdG/isdI nucleotide sequences were used for this tBLASTx search and amino acid sequences associated with tBLASTx hits that had an E-value hat $^{-05}$ were retrieved. Retrieved amino acid sequences were further screened by removing all sequences lacking the IsdG catalytic triad or a functional annotation. We also searched UniProt for all reviewed Isd proteins with known heme oxygenase function. A single representative operational taxonomic unit from each retrieved species was used to reconstruct the tree.

Prior to tree building, amino acid sequences were aligned with MUSCLE [52]. The final aligned dataset had 22 IsdG-family amino acid sequences of length 133. The Isd phylogeny was reconstructed using maximum likelihood (ML) [53]. The best fit model of amino acid substitution used in the ML reconstruction was determined with ProtTest 2.4 [54]. According to the AIC, the best fit substitution model was WAG+I+G+F [55]. The ML tree was reconstructed with PhyML 3.0 [56, 57] by maximizing the topology likelihood of ten random starting trees from the best of NNI and SPR branch rearrangements. The

gamma shape parameter (four rate categories) and proportion of invariable sites were

optimized via ML. Amino acid equilibrium frequencies were set at empirical levels. Node

statistical support was determined using a non-parametric bootstrap with 500 replicates.

Results

S. lugdunensis encodes an Isd system

S. lugdunensis requires iron for growth and can use heme to satisfy this requirement. This suggests that systems dedicated to the acquisition of heme are encoded within the *S. lugdunensis* genome. Using the nucleotide sequences of the *S. aureus isd* operon as queries, a putative Isd system was identified in *S. lugdunensis*. The *S. aureus,* Isd system encodes for 10 genes that work in concert to bind hemoglobin, remove the heme cofactor, and transport heme into the cell where it is degraded to release nutrient iron. Several proteins of the *S. aureus* Isd system are conserved within *S. lugdunensis* but important differences exist (Figure 2). For example, the Isd system of *S. lugdunensis* does not encode an *isdA* gene but rather an *isdA*-like gene, *isdJ,* which has two heme binding NEAT domains as opposed to the single NEAT domain of *S. aureus isdA.* Additionally, the *S. lugdunensis* Isd system encodes for a putative ABC transporter, *SLGD_00070* not present in the *S. aureus* Isd system. Moreover, the *S. aureus* Isd system utilizes two heme oxygenases, IsdG and IsdI, while the *S. lugdunensis* Isd system appears to utilize a single heme oxygenase. We refer to the *S. lugdunensis* heme oxygenase as IsdG in keeping with it being 68% identical to the amino acid sequence of *S. aureus* IsdG. Importantly, the catalytic triad (N6, W67, H76) shown to be critical for the enzymatic function of *S. aureus* IsdG [58] is conserved within the *S. lugdunensis* IsdG (Figure 2B). Analysis of the region upstream of the *S. lugdunensis isdCDEFSLGD_00070srtBisdGpghI* transcriptional start site revealed sequences with a high degree of similarity to consensus Fur box sequence from *S. aureus* (Figure 2C). Fur boxes are nucleotide sequences to which the iron-dependent repressor Fur binds. The presence of putative Fur boxes indicates that these

genes are likely iron-regulated, becoming maximally expressed in iron deplete conditions. These results suggest that *S. lugdunensis* encodes an iron-regulated Isd system including an IsdG family heme oxygenase.
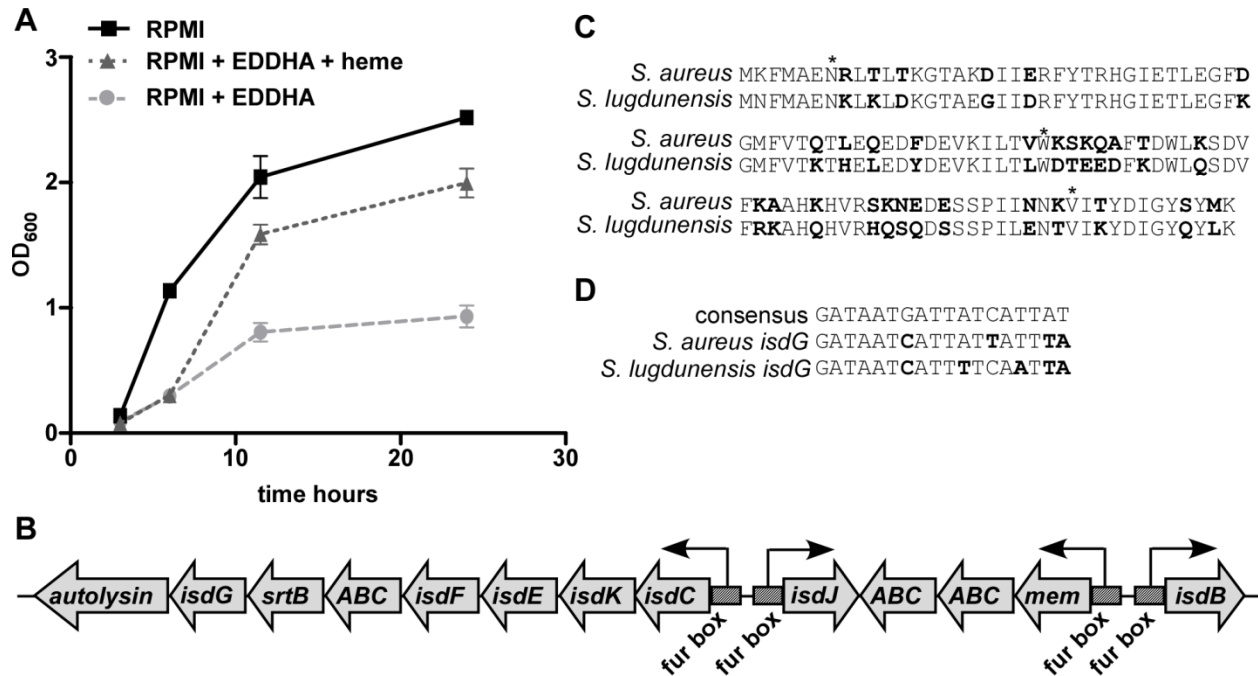
Figure 2. Sequence analysis of the *S. lugdunensis Isd* operon

(A) Growth comparison of *S. lugdunensis* grown in media alone, iron-depleted media or iron-depleted media supplemented with 5 μM heme. (B) The genomic organization of the isd locus within *S. lugdunensis* with four predicted transcriptional start sites designated by bent arrows. Putative Fur binding sites are marked by hashed boxes. All assignments are based on the annotated *S. lugdunensis* genome N920143 (in press with the accession number FR870271). (C) Amino acid alignment of *S. aureus* IsdG and *S. lugdunensis* IsdG with non-conserved amino acids shown in bold. Amino acids within the conserved catalytic triad are indicated with an asterisk. (D) Nucleotide sequence alignment of the *S. aureus* Fur box consensus sequence, *S. aureus isdG* Fur box sequence and the *S. lugdunensis isdG* Fur box sequence. Nucleotides that differ from the consensus sequence are shown in bold

S. lugdunensis IsdG binds and degrades heme

Heme binding proteins have a distinct absorption spectrum defined by peak absorbance in the range of 390-430 nm referred to as the Soret band. *S. lugdunensis* IsdG purified from *Escherichia coli* does not exhibit absorption patterns indicative of a heme binding protein. Reconstitution of IsdG with heme produces an optical absorption spectrum with a peak absorbance at 413 nm which incrementally increases upon addition of heme (Figure 3A). The Soret peak of heme-protein complexes is distinct from that of free heme at a neutral pH. This difference allows for the spectrophotometric titration of IsdG with heme from which the stoichiometry of IsdG and heme can be determined. Heme added incrementally to purified IsdG (10 µM) has a discrete inflection point at approximately 10 µM heme, indicating a 1:1 stoichiometry of protein and heme (Figure 3A inset). Together these data establish *S. lugdunensis* IsdG as a heme binding protein.

The ability of *S. lugdunensis* IsdG to degrade heme was evaluated using optical absorption spectroscopy. Purified recombinant IsdG was incubated with heme allowing protein heme complexes to form and monitored spectrophotometrically upon the addition of the electron donor ascorbate. Spectral analysis of the reaction was performed prior to the addition of ascorbate as well as at 15, 30, 60, 90 and 120 minutes [58] following the addition of ascorbate. This reaction resulted in almost complete elimination of the peak at 413 nm indicating opening of the macrocyclic conjunction of heme (Figure 3B). To distinguish between the coupled oxidation of heme and IsdG-mediated heme degradation all reactions were performed in the presence of catalase. These results demonstrate that *S. lugdunensis* IsdG catalyzes the oxidative degradation of heme in the presence of an electron donor.

A defining characteristic of IsdG-family heme oxygenases is the presence of an NWH catalytic triad required for heme catabolism [58]. We evaluated the functional requirement for these three residues in *S. lugdunensis* IsdG using mutational analysis. Each residue within the predicted catalytic triad was mutated to alanine and the heme binding properties of purified mutant proteins was assessed. All three mutant proteins (N7A, W67A, and H77A) retained the ability to bind heme indicating that these mutations do not disrupt the overall fold or heme binding properties of IsdG. However, inactivation of any residue within the catalytic triad resulted in the ablation of enzymatic function as demonstrated by the retention of the peak at 413 nm following addition of electron donor (Figure 4). These results indicate that IsdG enzymatically degrades heme through the catalytic NWH triad.
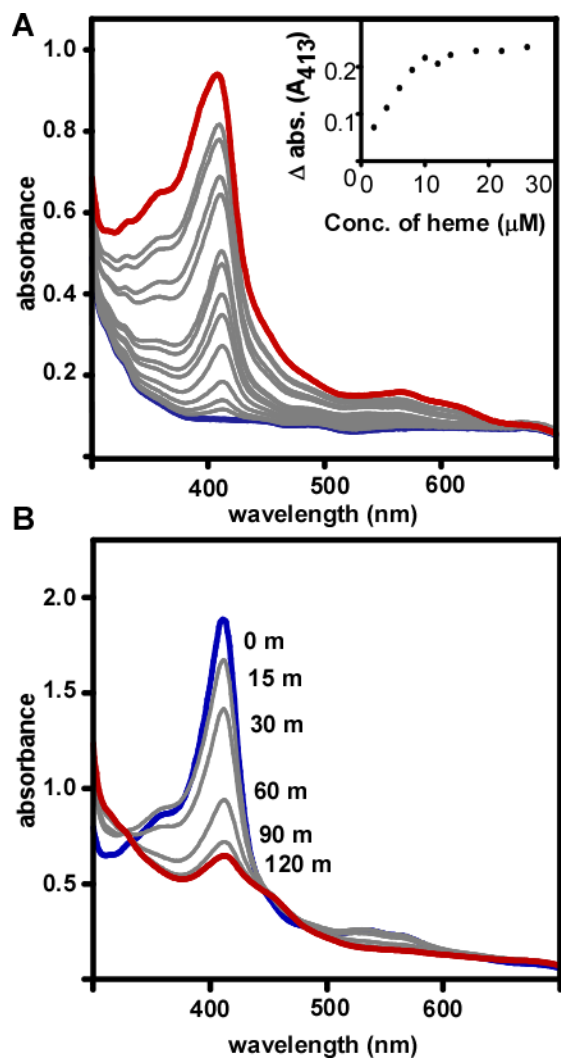
Figure 3. *S. lugdunensis* **IsdG binds and degrades heme.**

(A) Increasing amounts of hemin (2-40 µM) were added to a sample of purified IsdG (10 µM) and to a reference sample. Difference in absorbance of protein heme complex and free hemin at 413 nm is plotted against total heme concentration. Ten µM sample of protein was used (Inset). (B) Forty µM IsdG-heme complex after the addition of ascorbate (1 mM), spectra were taken at 0 (shown in blue), 15, 30, 60 and 90 minutes (shown in red). Reactions were performed in the presence of catalase at a 0.5:1 (catalase-hemoprotein) molar ratio.
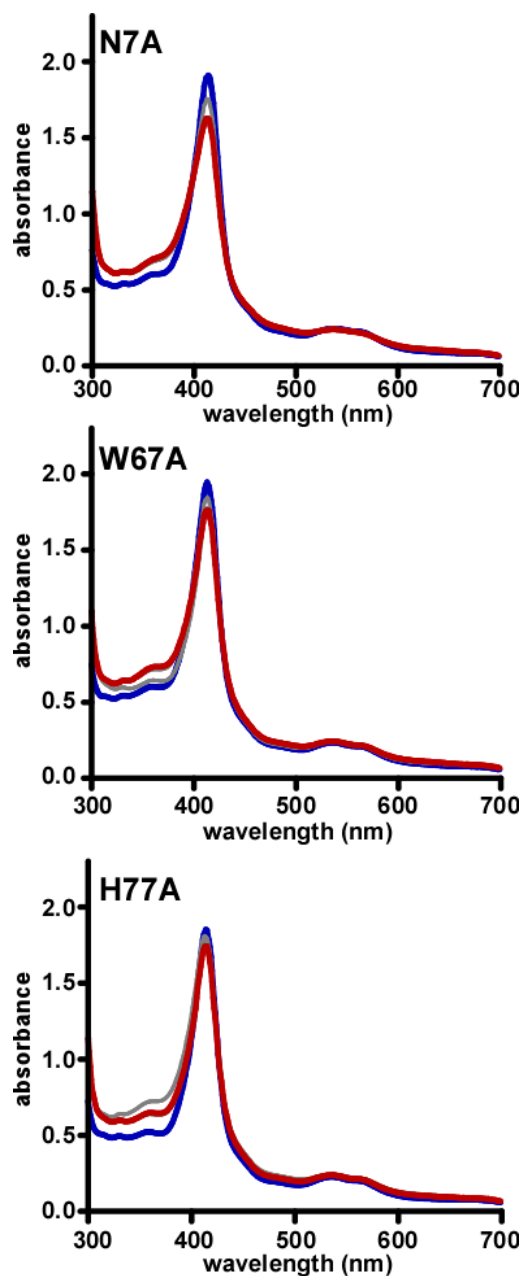
Figure 4. Catalytic triad is functionally conserved in *S. lugdunensis* IsdG.

Point mutants were made within the NWH catalytic triad by converting each of the three amino acids to alanine. Proteins were expressed and purified similar to wildtype and assessed for enzymatic activity. Forty μM IsdG-heme complex after the addition of ascorbate (1 mM), spectra were taken at 0 (shown in blue), 15, 30, 60 and 90 minutes (shown in red).

S. lugdunensis IsdG is iron-regulated

To ensure proper metal homeostasis, bacteria strictly regulate the uptake and metabolism of metals from the environment. A putative Fur-binding sequence is present upstream of the predicted operon encoding *isdG* suggesting that *isdG* is up-regulated upon iron starvation (Figure 2C). To test this hypothesis we employed immunoblotting to assess relative IsdG quantities within cells grown in increasing concentrations of the iron chelator 2,2,' dipyridyl (Dip). These experiments revealed that the relative abundance of IsdG increases expression in iron deplete conditions establishing IsdG as an iron-regulated enzyme (Figure 5A).

S. aureus encodes two IsdG-family enzymes, IsdG and IsdI, which are differentially regulated in response to iron and heme [34]. IsdI is maximally expressed in iron deplete conditions while IsdG is most abundant in iron deplete conditions in the presence of its substrate, heme. We therefore sought to determine what effect heme exposure has on IsdG levels within *S. lugdunensis* using quantitative immunoblotting. *S. lugdunensis* was grown in iron deplete conditions supplemented with increasing amounts of heme and IsdG levels were quantified (Figure 5B). This experiment revealed that the presence of heme has no effect on the intracellular abundance of IsdG within *S. lugdunensis.* Together these experiments show that *S. lugdunensis* IsdG is up-regulated in iron deplete conditions and is unaffected by the presence of heme. This is consistent with a model whereby *S. lugdunensis* up-regulates its heme catabolizing machinery during times of nutrient iron starvation.
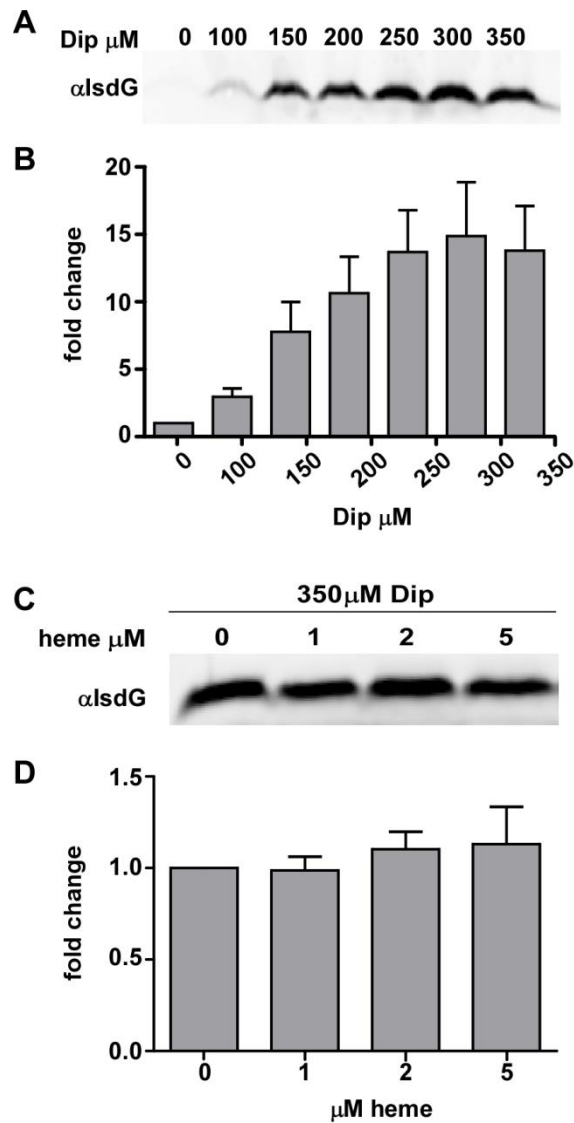
Figure 5. *S. lugdunensis isdG* is iron-regulated.

S. lugdunensis was grown overnight with the indicated supplements and protoplasts werelysed and normalized by total protein concentration. (A and B) Effect of iron chelation by 2, 2, dipyridyl (Dip) on IsdG expression level analyzed by immunoblot. Fold change in cytoplasmic IsdG levels in increasing concentrations of Dip as compared to IsdG levels in media alone. (C and D) Effect of exogenous heme on expression of IsdG when grown in iron-depleted media analyzed by immunoblot. (D) Fold change in IsdG levels from cells grown in iron-depleted media with increasing concentrations of exogenous heme as compared to IsdG levels from cellsgrown in iron-depleted media alone.

S. lugdunensis IsdG degrades heme to staphylobilin

Two structurally distinct families of heme oxygenases have been identified, the HO-1 family and the IsdG family. While the HO-1 family of heme oxygenases is ubiquitous across Kingdoms the IsdG family has only been identified in bacteria. The mechanism of heme degradation in the HO-1 family is highly conserved and typically results in the production of the blue-green molecule α-biliverdin [59]. Within eukaryotes biliverdin is further reduced to the yellow molecule α-bilirubin by biliverdin reductase [60]. In contrast, IsdG family members within *Staphylococci* degrade heme directly to yellow oxo-bilirubin molecules that have been named staphylobilins [32]. Based on this, we sought to determine the identity of the product of IsdG-mediated heme degradation within *S. lugdunensis*. Initially, we analyzed the product of IsdG-mediated heme degradation using high pressure liquid chromatography (HPLC) and compared its retention time to that of staphylobilin, and biliverdin (Figure 6). When analyzed by HPLC the heme degradation product generated by *S. lugdunensis* IsdG eluted in a series of two peaks with a retention time identical to that of staphylobilin (Figure 6). Importantly, the heme degradation product of *S. lugdunensis* IsdG eluted earlier than either biliverdin or bilirubin indicating a higher degree of polarity (Figure 6). After HPLC purification the products of *S. lugdunensis* and *S. aureus* IsdG mediated heme degradation were subjected to high resolution electrospray ionization mass spectrometry (HRESIMS). This analysis allowed for the molecular composition of each peak to be determined and subsequently compared. Samples from both peaks resulted in products with a mass of 598.25 Da (*m/z* 599.2605 [M+H] Δ = 0.5-4.2 ppm) corresponding to a molecular formula of $C_{33}H_{34}N_4O_7$ (Figure 7) [32]. Importantly, the molecular masses of biliverdin and bilirubin are 582.6 and 584.7 Da

respectively, and are clearly distinct from that of staphylobilin. Together these data indicate that *S. lugdunensis* IsdG degrades heme to staphylobilin.
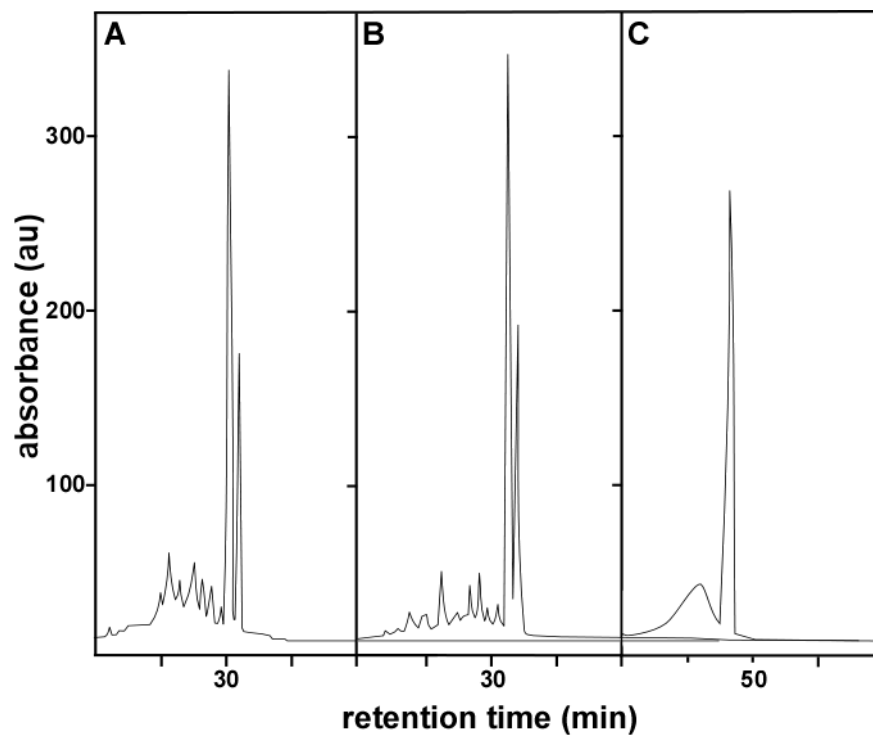
Figure 6. HPLC analysis of *S. lugdunensis* IsdG heme degradation product

HPLC comparison of established heme degradation products indicates that *S. lugdunensis* IsdG degrades heme to staphylobilin. (A) Staphylobilin purification monitored at 465 nm. (B) *S. lugdunensis* IsdG-mediated heme degradation product monitored at 465 nm. (C) Biliverdin purification monitored at 405 nm.
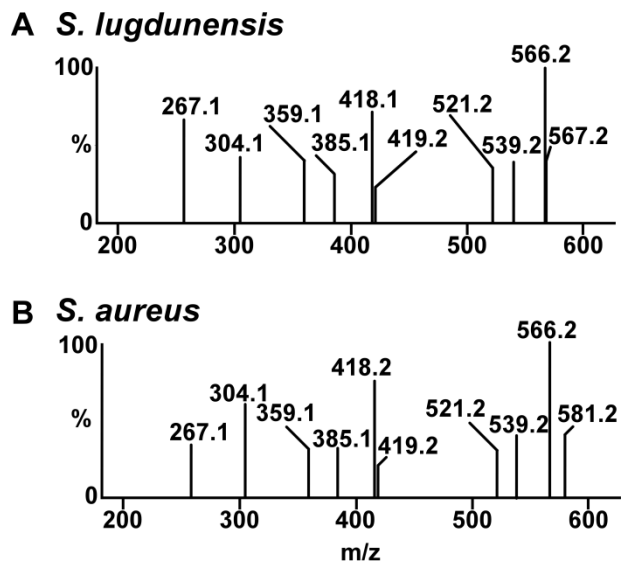
Figure 7. Tandem LC-HRESIMS analysis of *S. aureus* staphylobilin and *S. lugdunensis* IsdG heme degradation product

(A) ESI-MS/MS of fragment ions selection for 599.3 *m/z* for *S. lugdun*ensis IsdG-mediated heme degradation products. (C) ESI-MS/MS of fragment ions selection for 599.3 *m/z* for *S. aureus* IsdG-mediated heme degradation products.

***S. lugdunensis* IsdG facilitates the use of heme as an iron source**

Heme degradation results in the release of free iron for use as a nutrient source. To determine the biological function of *S. lugdunensis* IsdG we measured the ability of *S. lugdunensis* IsdG to complement the heme utilization defect of the *S. aureus* heme oxygenase mutant (*ΔisdGI*) [35]. Heme utilization was measured by comparing the growth of plasmid containing strains of *S. aureus* in iron deplete medium supplemented with heme. To eliminate complications associated with iron-dependent effects on transcription, *isdG* was cloned into the p-OS1*plgt* vector resulting in the constitutive expression of *isdG* under the *lgt* promoter [51]. Expression of *S. lugdunensis* IsdG completely restored the ability of *S. aureus ΔisdGI* to utilize heme as an iron source for growth (Figure 7). In fact the complemented strain grew better than wildtype at early time points demonstrating that overexpression of IsdG provides an enhanced ability to grow on heme as a sole source of iron. These results indicate that *S. lugdunensis* IsdG degrades heme to release free iron and enhance bacterial growth.
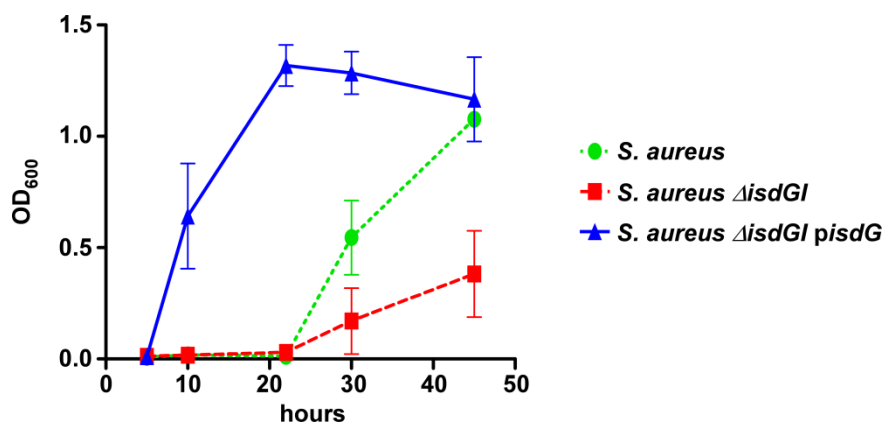
Figure 8. *S. lugdunensis* **IsdG complements the heme utilization defect of a** *S. aureus* **heme oxygenase mutant.**

Comparison of growth by plasmid containing strains of *S. aureus*, *S. aureus ΔisdGΔisdI*, and *S. aureus ΔisdGΔisdI* complemented with *S. lugdunensis isdG*. Strains were grown in minimal media with hemin supplemented as the only iron source.
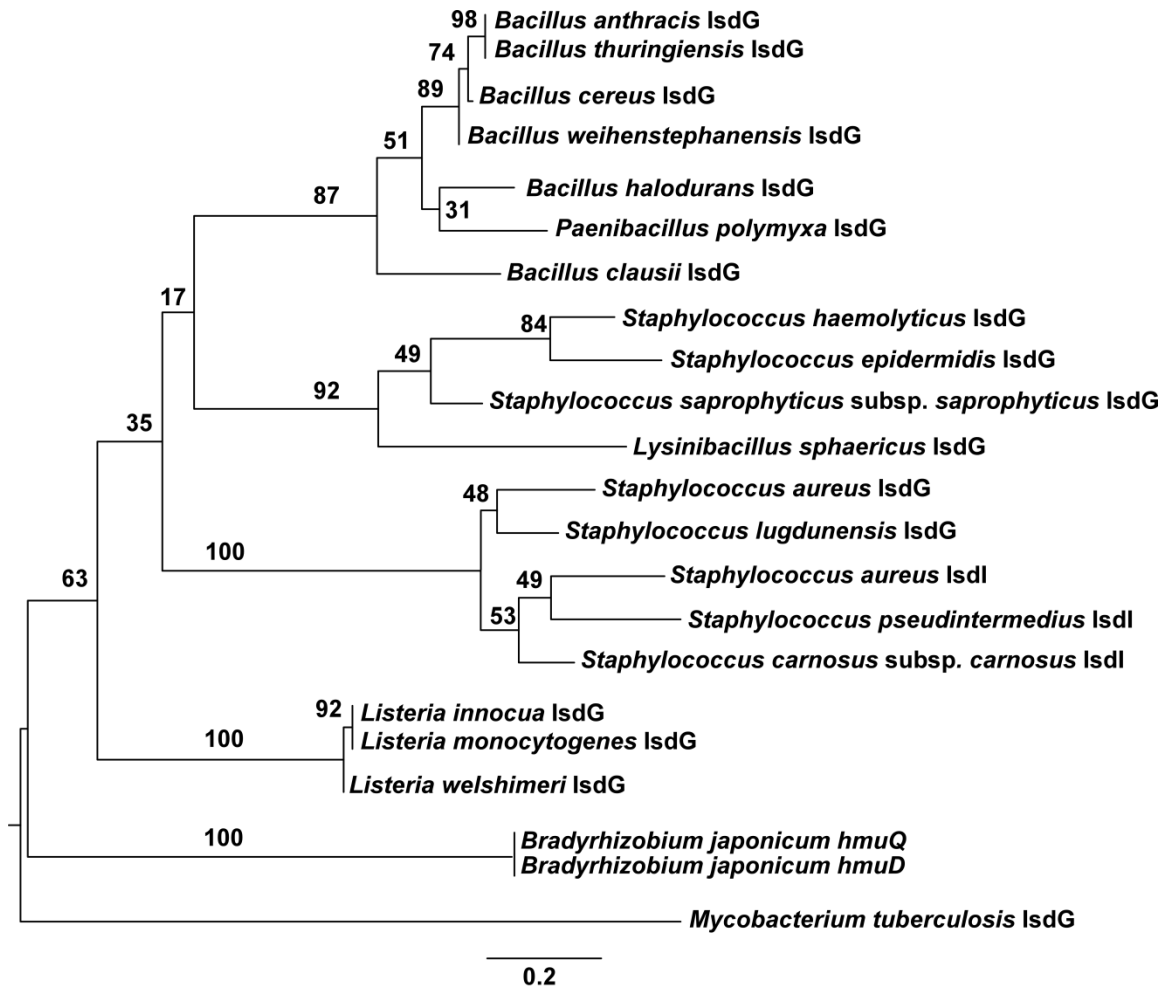
Figure 9. Two distinct Staphylococcal clades within a phylogenetic tree of annotated IsdG-family heme oxygenases.

Midpoint rooted phylogenetic tree of IsdG/I amino acids sequences from bacterial taxa with characterized heme oxygenases. The phylogeny was reconstructed using maximum likelihood (ML) and the tree with the highest log likelihood (lnL = -3131.92126) is shown. A non-parametric bootstrap (500 replicates) was used to determine node support. Bootstrap values are shown at each node. Branch lengths are to scale and measured in amino acid substitutions per site.

Discussion

While the types of infections caused by *S. lugdunensis* are well described, the molecular mechanisms employed during infection have not been identified. As with most bacterial pathogens, *S. lugdunensis* cannot survive and replicate in the absence of iron. Moreover, free iron within host tissues is found at concentrations significantly less than is required to sustain bacterial growth [46, 61]. To combat this barrier to growth, *S. lugdunensis* presumably encodes systems dedicated to the acquisition of nutrient iron during infection. Consistent with this, we report here that *S. lugdunensis* encodes an Isd system including an IsdG family heme oxygenase that degrades heme to staphylobilin and free iron. IsdG is up-regulated during conditions of iron starvation ensuring that the heme catabolizing machinery is abundant during times of nutrient stress. Furthermore, *S. lugdunensis* IsdG promotes growth of a *S. aureus* heme oxygenase mutant on heme supporting the placement of this enzyme within the heme-iron acquisition pathway. Based on these findings, it is likely that the *S. lugdunensis* Isd system is utilized in low iron conditions to bind host hemoproteins, remove heme and transport it into the cytoplasm where it can be degraded to release free iron. Functional IsdG family heme oxygenases have been identified in *S. aureus*, *Bacillus anthracis*, *Bradyrhizobium japonicum*, *B. melitensis*, and *Mycobacterium tuberculosis* [35, 47, 62, 63]. To gain insight into the evolutionary relationships between these IsdG family members we interrogated all bacterial genomes to identify IsdG orthologs and created a phylogenetic tree using all annotated IsdG family members (Figure 9). Interestingly, Staphyloccocal IsdG members segregated into two distinct clades with *S. aureus* and *S. lugdunensis* in the same clade and *S. epidermidis* and *S. haemolyticus* in a separate clade (Figure 9). Additionally, *S. aureus* IsdG is more closely related to *S. lugdunensis* IsdG than to any other IsdG family

member including its paralog, IsdI. Moreover, our analysis of all sequenced bacterial genomes revealed predicted IsdG orthologs across diverse classes of bacteria such as *Alphaproteobacteria, Agrobacterium, Actinobacteria, Betaproteobacteria, Chloroflexi, Corynebacterinaea and Deinococcus-Thermus*. The broad conservation of IsdG across diverse classes of bacteria implicates heme degradation as a primary mechanism by which bacteria meet their iron requirements. Although the use of IsdG to catabolize heme may be pervasive among bacteria the number of species with putative IsdG heme oxygenases suggests that many questions remain regarding this enzyme. For example, many species with a predicted IsdG heme oxygenase have no known association with any plant or animal from which they could acquire heme. These species including *Salinispora tropica*, *Oligotropha carboxidovorans*, and *Thermus thermophiles* occupy unique niches, thriving in inhospitable environments such as thermal hot springs. Upon further investigation of the genomes of these bacteria it was discovered that they all possessed the necessary genes to synthesize heme endogenously. Therefore these bacteria may encode an IsdG family heme oxygenase to allow for the production of staphylobilin, adding support to the hypothesis that staphylobilin has an important biological function.

The *S. aureus* Isd system includes three cell wall anchored proteins IsdA, IsdB and IsdC all of which are capable of binding heme. [64]. Putative orthologs of both IsdB and IsdC have been identified within the *S. lugdunensis* Isd system. Additionally, the *S. aureus* Isd system encodes for IsdD (a membrane protein), IsdF (a polytopic transmembrane protein) IsdE (a lipoprotein ATPase) and a sortase, SrtB, responsible for anchoring IsdC to the cell wall [64, 65] and

these proteins with the exception of IsdD are conserved within the *S. lugdunensis* Isd system. However, important differences between the two operons exist. One difference is the putative ABC transporter within the *S. lugdunensis* Isd system situated between *isdF* and *srtB.* This ABC transporter may be involved in iron homeostasis as its location within the predicted Isd operon suggests that it is iron regulated. Additionally it may facilitate heme uptake by acting as an accessory protein to the IsdEF heme transporter. While the *S. lugdunensis* Isd system does not include IsdA, it does encode for an additional wall anchored protein IsdJ. The role of IsdJ in iron acquisition has not been elucidated, however it does have two predicted NEAT domains and binds heme indicating it may be functionally analogous to *S. aureus* IsdA [36]. Another key difference between the two Isd systems is the presence of IsdI, an IsdG paralogue present in *S. aureus* but not *S. lugdunensis*. These two heme oxygenases have been shown to be differentially regulated within *S. aureus* [34]. Both heme oxygenases are transcriptionally regulated by Fur in response to iron levels however in the absence of heme IsdG is targeted for proteolytic degradation [34]. The biological significance of this differential regulation is not fully understood. One possibility is that by differentially regulating IsdG and IsdI, *S. aureus* can more precisely regulate heme degradation levels. *S. aureus* gains access to host heme through the expression of hemolysins which lyse erythrocytes. *S. aureus* regulates hemolysin expression in response to bacterial density by the global virulence regulator, *agr.* The two heme oxygenases within *S. aureus* may function such that IsdI is required early in infection to degrade the small amount of available heme present prior to the secretion of hemolysins. After seeding of host organs hemolysin expression likely increases resulting in an influx of heme necessitating the need for a second heme

oxygenase, IsdG. A single iron regulated heme oxygenase may be sufficient within *S. lugdunensis* because the amount of heme available for degradation may be more consistent throughout infection. This model is supported by the finding that hemolytic activity due to α, β or γ-hemolysins has not been detected in *S. lugdunensis* [7]. Additionally, most isolates of *S. lugdunensis* have been found to produce a δ-like hemolysin comprised of three 43-amino acid peptides encoded not in the *agr* locus but the SLUSH locus [14]. The location of these genes outside the *agr* locus suggests that they are regulated by an as-yet-determined mechanism. Consequently, cytoplasmic heme levels within *S. lugdunensis* may not vary considerably throughout the course of infection, and regulating IsdG through Fur alone may allow for sufficient control of the heme catabolizing machinery within the cell. Another potential explanation for regulating intracellular levels of IsdG through iron alone is that the *S. lugdunensis* Isd system may be less efficient than that of *S. aureus* resulting in comparatively lower cytoplasmic heme concentrations during infection. The amount of heme entering the cell may not allow for the heme dependent stabilization of an IsdG family heme oxygenase.

S. *lugdunensis* IsdG degrades heme to staphylobilin (Figures 7 and 8). This is the first evidence that the production of staphylobilin is conserved amongst IsdG family members within *Staphylococci*. Bilirubin, biliverdin and carbon monoxide are the products of vertebrate heme catabolism and all of these molecules have important functions within mammalian cells [66]. For example, biliverdin and carbon monoxide both have beneficial anti-inflammatory functions and all three molecules act as anti-oxidants within the serum [66, 67].The biological roles of heme degradation products within bacteria remain unknown. Bacterial HO-1 family heme oxygenases degrade heme to biliverdin however

a biliverdin reductase ortholog has not been identified in bacteria. Furthermore, it remains unclear if bacterial derived biliverdin has a physiological function. Carbon monoxide is produced during heme catabolism by HO-1 family heme oxygenases while IsdG family heme oxygenases produce formaldehyde [66, 68]. It is plausible CO production by HO-1 or formaldehyde production by IsdG family enzymes affects bacteria, however the impact of the endogenous synthesis of these molecules has yet to be determined. Establishing staphylobilin as a conserved Staphylococcal heme degradation product supports the idea that this molecule may serve a valuable biological function within pathogenic bacteria.

This work has established the role of *S. lugdunensis* IsdG in heme-iron utilization and identifies the first gene within *S. lugdunensis* involved in nutrient acquisition. IsdG mediated heme degradation is required for full virulence within *S. aureus* [34]. *S. aureus* strains lacking *isdG* or *isdI* are severely attenuated for growth within murine hearts following systemic challenge [34]. This work supports the idea that bacterial heme degradation is vital to cardiac colonization. Future experiments will aim at elucidating the contribution of IsdG to the virulence of *S. lugdunensis* during the pathogenesis of endocarditis. The significant structural differences between IsdG family members and human HO-1 heme oxygenases highlights the potential to therapeutically target IsdG. Further investigation of the contribution of the Isd system to *S. lugdunensis* pathogenesis may facilitate the development of Isd directed antimicrobials.

Chapter III

THE *S. LUGDUNENSIS* ISD PEPTIDOGLYCAN HYDROLASE MODULATES ISDC RELEASE AND FACILITATES BIOFILM FORMATION

Introduction

Staphylococcus lugdunensis is a common skin commensal that is gaining more recognition as a clinically relevant pathogen due to its propensity for causing aggressive and rapidly progressive infections. *S. lugdunensis* is frequently associated with infections linked to biofilm formation such as endocarditis, and prosthetic joint infection, however little is known regarding the molecular mechanisms that facilitate *S. lugdunensis* adherence and biofilm regulation. In fact, only two *S. lugdunensis* proteins to date have been shown to mediate bacterial adherence. The fibrinogen binding protein Fbl is highly related to clumping factor A (ClfA) of *S. aureus* which contributes to endocarditis in a *S. aureus* rat model of infection [12, 69]. Importantly, *S. lugdunensis* strains lacking a functional *fbl* gene are unable to bind to fibrinogen. The second protein is vWbp which is conserved in *S. lugdunensis* and facilitates the establishment of infectious legions in a *S. aureus* infection [13, 70].

Bacteria encode for multiple peptidoglycan (PG) hydrolases which are involved in a variety of biological functions including cell wall turnover, cell separation, and antibiotic-induced autolysis. Additionally, many PG hydrolases contribute to the pathogenesis of Gram positive pathogens through innate immune modulation and biofilm formation. This fact is underscored by the numerous species of bacteria including *Streptococcus*

pneumonia, Staphylococcus epidermidis and Listeria monocytogenes in which a PG hydrolase mutant has a virulence defect [70-73].

The Isd system within *S. lugdunensis* clearly plays a role in iron acquisition however some genes that are unique to the *S. lugdunensis* operon have roles that have yet to be elucidated, specifically, the terminal gene *pghI*, a predicted PG hydrolase. In this study I show that *pghI* is part of the *S. lugdunensis* Isd system and consequently is iron regulated. Additionally I demonstrate that PghI has PG hydrolyzing activity and that PghI modulates the release of the wall anchored IsdC protein. Furthermore, I show that both IsdC and PghI are involved in biofilm formation.

Methods

RNA isolation

Overnight cultures of wildtype *S. lugdunensis* were subcultured (1:100) in triplicate into tryptic soy broth (TSB) alone or TSB with 350 µM Dip. Midlog cultures (O.D. 600 = 0.3) were then harvested and mixed with an equal volume ethanol and acetone (1:1 ratio) and stored at -80°C. For RNA extraction samples were then thawed on ice and cells pelleted by centrifugation 8,000 X g for 10 min. Pellets were then resuspended in LETS buffer (1 M LiCl, 0.5 EDTA, 1 M Tris-HCl, pH 7.4, 10% SDS) and lysed in lysing matrix B tubes (MP Bio) agitated in a FastPrep Instrument (MP Bio) set at 6 m/s for 45 s. Samples were heated to 55°C for 5 min and then centrifuged at 16,000 X g for 10 min. RNA was isolated by removing supernatants and mixing with 1.0 mL TRIzol (Tri Reagent; Sigma), and incubating the mixture at room temperature for 5 min. Chloroform was added to samples (200 µL) and then samples were vigorously shaken for 15 s, incubated at room temperature for 2 min and then centrifuged at 16,000 X g for 15 min. RNA was extracted by removing the top aqueous fraction, mixing it with 1 mL isopropyl alchohol, and incubating the samples at room temperature for 10 min. Samples were centrifuged at 16,000 X g for 10 min, pellets were washed with 1 mL 70% ethanol, and air dried for 1 m. RNA was then resuspended in 100 µL of distilled water and contaminating DNA was removed by the addition of 10 µL of DNaseI (Amersham Bioscience) and RQ1 buffer (Promega) and then incubating at 37°C for 30 min. After the removal of DNA, samples were cleaned using an RNeasy minikit (Qiagen) according to manufacturer's protocol.

Real-time reverse transcription PCR (RT-PCR)

For cDNA synthesis, 2 µg of total cellular RNA was reverse transcribed using Moloney murine leukemia virus (M-MLV) transcriptase according to the manufacturer's protocol (Promega). cDNA was amplified in triplicate using iQ SYBR green Supermix (Bio-Rad) in an iCycler iQ instrument (Bio-Rad). Quantification of each sample was determined relative to 16S rRNA. Statistical significance was determined using Student's *t* test.

Protein purification

Recombinant *S. lugdunensis* PghI was purified from *Escherichia coli* BL21 (DE3) carrying the pET-15b-*isdG* plasmid. Overnight cultures were grown at 37º in TSB with 100 µg/ml ampicillin and 34 µg/ml chloramphenicol. The next day cells were diluted in fresh media and grown to mid-log phase at which time expression was induced through the addition of 1mM isopropyl-1-thiol-(D)-galactopyranoside. Cell growth continued for 3 H at 30º after which time cells were collected through centrifugation at 8,000 x *g* for 10 min. Cell pellets were then washed with 50 mM Tris-HCl (pH 7.5) 100 mM NaCl, collected through centrifugation and stored at -80º. To collect recombinant protein cells were thawed on ice and resuspended in 50 mM Tris-HCl (pH 7.5) 100 mM NaCl with 100 µM phenylmethylsulfonyl fluoride. Cells were lysed using a French press and the cell suspension was centrifuged at 100,000 x *g* for 60 min. After centrifugation the soluable fraction was filter through a 0.45 µm filter and then applied to a Ni-Nitrilotriacetic acid column that had been pre-equilibrated with 50 mM Tris-HCl (pH 7.5), 100 mM NaCl. The column was then washed with two volumes of 50 mM Tris-HCl (pH 7.5) 100 mM NaCl followed by a wash using three volumes of 50 mM Tris-HCl (pH 7.5), 100 mM NaCl with

10% glycerol and 10 mM imidazole. Protein was eluted with 50 mM Tris-HCl (pH 7.5), 100 mM NaCl containing 500 mM imidazole. Proteins were then dialyzed against 50 mM Tris-HCl (pH 7.5), 100 mM NaCl. Protein concentrations were determined using a BCA assay and purity was evaluated by SDS-PAGE.

Peptidoglycan purification

Overnight cultures of Δ*pghl* were subcultured (1:100) into 1 L of TSB with 350 µM Dip. Cells were grown to stationary phase (O.D.=5.0) and pelleted through centrifugation at 6,000 X *g* for 10 min. Cells were then resuspended in 100 mL of 4% SDS and boiled for 20 min. Saculli were collected through centrifugation at 6,000 X *g* for 10 m, washed five times with 50 mL of distilled water, and washed two times with 50 mL acetone. Saculli were then incubated overnight at 37°C to remove any remaining acetone. Peptidoglycan was removed from saculli by resuspending in 20 mL of ice cold distilled water with 15 mL silica beads and vigorously vortexed for 20 min. Peptidoglycan was isolated from the silica beads by centrifugation at 1,400 X *g* for 10 min and supernatants collected. Silica beads were washed until supernatants were clear and free of peptidoglycan. Unbroken cells were removed from the peptidoglycan prep by centrifugation at 4,000 X *g* for 10 min and the supernatant fraction collected. Peptidoglycan was pelleted by centrifugation at 8,000 X *g* for 30 min. DNA and RNA contamination was removed from the peptidoglycan by adding 120 U of DNase and 50 U of RNase to sample suspended in phosphate-buffered saline (PBS) and incubate at 37°C for 18 H. Protein contamination was removed through proteinase K treatment. 4.0 mg of proteinase K was added to each sample and incubated at 37°C for 18H. Sample was then pelleted through centrifugation at 8,000 X *g* for 30 min and teichoic acid was removed through TCA precipitation. Sample was resuspended in

50 mL of 10% TCA and incubated at 4°C for 18 H. The sample was then pelleted and resuspended again in 50 mL of 10% TCA and incubated a second time at 4°C for 18 H. Sample, which is purified PG was then pelleted through centrifugation at 8,000 X *g* for 30 min and washed three times in 50 mL of water. After washing purified PG is lyophilized and stored at -20°C until ready to use.

Zymogram assay

The zymogram assay was done by running 30 µg recombinant protein onto a 15% acrylamide gel which had 1mg purified peptidoglycan added to the gel and then performing SDS-PAGE. The acrylamide gel was then washed three times with 50 mL of distilled water before incubating in re-naturing buffer (10 mM Tris buffer, 0.1% TritonX100 pH 5.0-8.0) at room temperature for 48 H. Precipitated protein was removed from gels by incubating them in a 10% SDS buffer for 3 H. Gels were stained with a 1% methylene blue in 0.01% KOH solution to increase contrast.

Biofilm assay

A 96 well flat bottom plate was prepared for the biofilm assay by adding 150 µL of 20% bovine plasma to each well. The plate is incubated at 4°C overnight and then the plasma was removed. Next, 150 µL of TSB with 350 µM Dip was added to the wells and then inoculated with 1.5 µL of overnight culture. Overnight cultures were grown in 100 µL of media in a 96 well plate and each well was inoculated with a single colony and grown overnight at 37°C with shaking. Biofilm plates were set up in duplicate with one plate being used to measure biomass and the other to measure biofilm formation. After the plasma treated plates were inoculated the plates incubate at 37°C without shaking for 48 H. To

determine biomass, biofilms were disrupted from one plate by vigorous pipetting and 20 µL transferred into 180 µL of PBS in a 96 well plate and O.D. 600 taken. To measure biofilm production media was removed from wells and then wells were washed three times with 200 µL of PBS. Next 200 µL of ethyl alcohol was added to each well to fix the biofilm. After the ethyl alcohol was removed the plate was dried at room temperature for a minimum of 1 H. Biofilms were stained for 15 min with 100 µL a 0.41% crystal violet solution in 12% ethyl alcohol. Wells were then washed three times with 200 µL of PBS and allowed to dry at room temperature for a minimum of 1 H. Excess crystal violet was removed by adding 200 µL of 33% acetic acid to each well and incubate at room temperature for 30 m. Acetic acid was removed and biofilm mass was determined by reading the O.D. at 598 nm. Assays were conducted with a minimum of three biological replicates.

Results

PghI is iron regulated

pghI is the terminal gene within the Isd operon and consequently is predicted to be co-transcribed with the upstream genes *isdC* through *isdG* in an iron-dependent manner such that transcription increases upon iron starvation (Figure 10B). To test this hypothesis I analyzed transcript levels of *pghI* in cells grown in iron rich media and iron deplete media. I observed that transcript levels of *pghI* increased nearly 70-fold upon iron starvation consistent with Fur regulation that has been previously established for the *S. lugdunensis* Isd operon (Figure 10A) [36, 37]. This level of up-regulation is comparable to that of *isdC*, the first gene within the operon. To confirm that *pghI* is co-transcribed along with the rest of the Isd operon, cDNA isolated from iron starved cells was used as template within a PCR reaction with a 5' primer located within the *isdG* gene and a 3' primer located within the *pghI* gene (Figure 9B). This PCR showed a positive amplicon band indicating that *isdG* and *pghI* are transcribed in the same continuous piece of mRNA (Figure 10B and C). Together these results along with the well-established iron dependent Fur-mediated regulation of Isd systems indicate that *pghI* is part of the Isd operon and is transcriptionally up-regulated upon iron restriction along with the rest of the Isd operon.
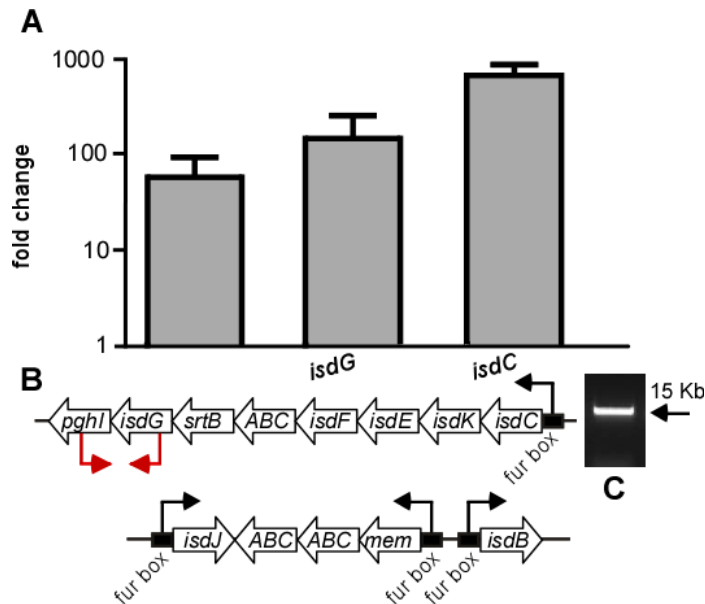
Figure 10. *pghI* is part of the Isd operon and is iron regulated

Transcript levels of *isdC, pghI* and *isdG* were analyzed by quantitative RT-PCR and normalized to 16S rRNA. Wild type *S. lugdunensis* was grown in iron-deplete media (TSB with 350 μM Dip) and transcript levels were compared with those grown in TSB. Error bars represent the average range of triplicate experiments (A). Genomic organization of the *S. lugdunensis* Isd locus with four predicted transcriptional start sites designated by black bent arrows. All assignments are based on the annotated *S. lugdunensis* genome N920143 (B)**.** PCR product generated using cDNA isolated from S. *lugdunensis* grown in iron deplete media. Primers used to create amplicon are located within *pghI* and *isdG* and are designated by red bent arrows. Amplicon production indicates that *pghI* is part of the Isd locus and is transcribed together with *isdG* (C)*.*

PghI is a peptidoglycan hydrolase

Based on sequence alignments PghI is predicted to have peptidoglycan hydrolyzing activity through both a FlgJ domain, and C-terminal CHAP domain. The N-terminus of PghI contains a secretory sequence suggesting that it is secreted through the membrane by the Sec system. The N-terminus of PghI contains a predicted disordered domain of approximately 130 amino acids with no identifiable domains or homology (Figure 11A). Together this information lead me to hypothesize that PghI is a secreted PG hydrolase with both a FlgJ domain and a CHAP domain. To confirm the PG hydrolyzing ability of PghI I used a zymography assay using purified PG from *S. lugdunensis* cells grown in iron deplete conditions. The zymogram showed a zone of clearing at approximately 53 kDa corresponding to the size of PghI lacking a secretory signal. Zymograms were done with a range of pHs and I found that PghI shows the greatest activity at low pHs between 5.0-6.0 with no detectable activity at a pH of 8.0 or above (Figure 11).
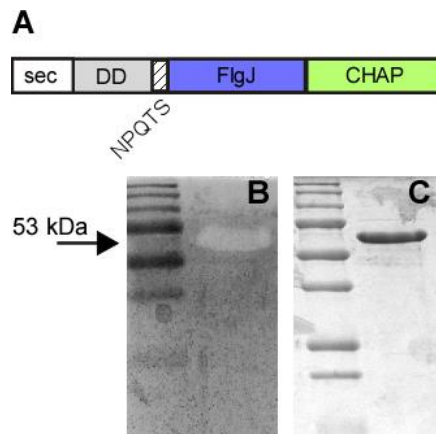
Figure 11. PghI is a peptidoglycan hydrolase

Graphical representation of PghI shows the location of a Sec signal, disordered domain (DD), putative sortase B sorting signal, FlgJ domain and CHAP domain (A). Peptidoglycan hydrolysis activity was assessed through a zymogram assay using SDS PAGE impregnated with PG purified from iron-starved Δ*pghI S. lugdunensis* cells (B). Recombinant PghI was run out on zymogram gel. Zones of clearing indicate PG hydrolase activity. Recombinant PghI was analyzed using SDS-PAGE to confirm size of protein (C).

PghI modulates the IsdC secretion profile of *S. lugdunensis*

The Isd system includes multiple wall anchored proteins that allow for the extraction of heme from hemoglobin and the subsequent transport of heme across the cell wall. This anchoring is achieved through the enzymatic activity of sortase A and sortase B which recognize substrates through either an LPXTG or NPQTS peptide motif, respectively, and then covalently link targeted proteins to the cell wall [39, 64, 74]. Proteins destined for sortase anchoring must first be exported through the membrane by the Sec secretion system and consequently these proteins have three sizes as they progress through the cell to ultimately be localized to the wall. Immediately after translation proteins are at their largest size referred to as P1. Upon passing through the Sec system and the subsequent removal of the Sec signal peptide proteins reduce in size resulting in the P2 form. Finally after sortase cleavage and subsequent PG linkage at the C-terminus of the protein the proteins reach their mature and smallest size referred to as M [74]. The wall anchored protein, IsdC is bound to the cell wall through sortase B [36].

Due to the location of *pghI* within the Isd operon and its peptidoglycan hydrolyzing activity I hypothesized that PghI modifies the PG wall to allow for proper placement of wall anchored Isd proteins. To test this hypothesis I pelleted cells from overnight cultures grown in both iron rich and iron deplete media through centrifugation and collected the supernatant fractions. Cells were then resuspended in TSM (100 mM Tris pH 7.0, 500 mM sucrose, 10 mM $MgCl_2$) and treated with lysostaphin to remove the cell wall. Next protoplasts were pelleted and the supernatants collected for the wall fraction. These fractions were then run on an agarose gel and proteins analyzed by silver stain. No differences could be seen in the wall fractions however; within the supernatant fractions

one protein band was present in wildtype but significantly reduced in the *ΔpghI* strain. The reduced band was approximately 18kD in size, corresponding to the mature size of IsdC, therefore I hypothesized that PghI was modulating the IsdC protein profile within the supernatant fraction. To test this hypothesis, supernatant fractions from wildtype *S. lugdunensis* and the *ΔpghI* strain grown in iron replete and iron deplete media were collected and run on an agarose gel. Proteins were then transferred to a nitrocellulose membrane and probed with anti-IsdC polyclonal antibodies. This immunoblot indicated that IsdC is present within the supernatant of wildtype cells in two different sizes and the larger band is significantly reduced within the *ΔpghI* mutant (Figure 12A and B).

As a sortase B substrate IsdC proceeds from the P1 to P2 and then to the M form as it progresses from the cytoplasm, through the membrane and is finally linked to the cell wall [75]. To elucidate where in this sorting process PghI is modulating IsdC release, I performed an immunoblot on *ΔsrtB* supernatants and found no detectable IsdC indicating that sortase B activity is required for IsdC release. Furthermore, when wildtype cells and *ΔpghI* were fractionated to separate cytoplasm, membrane, wall and supernatant fractions it was found that both wildtype and *ΔpghI* strains have the same amount and size of IsdC within the membrane and cytoplasm indicating that PghI does not influence sortase B activity or the amount of IsdC anchored to the wall (Figure 12C). Together these results indicate that PghI acts on IsdC after it has been anchored to the PG wall by sortase B and that PghI does not alter the amount of IsdC anchored to the wall.
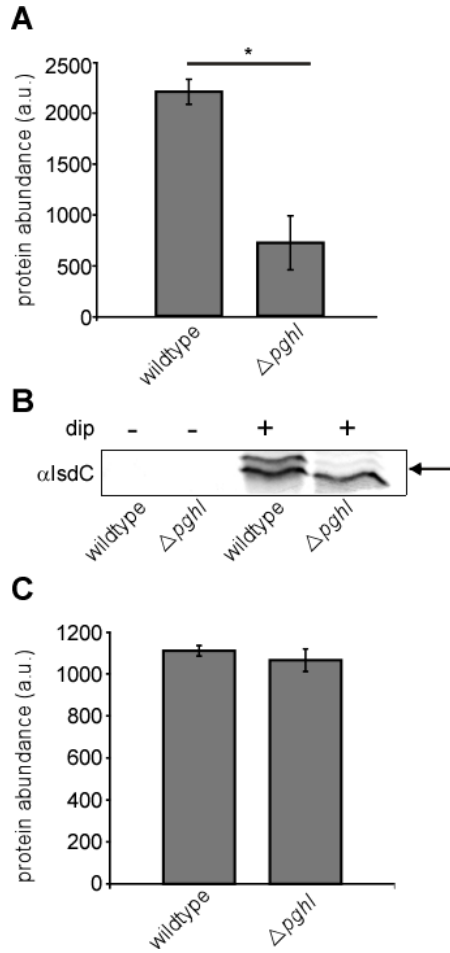
Figure 12. PghI modulates IsdC release into the extra-cellular milieu

Modulation of IsdC release from the cell wall into the supernatant by PghI was measured using quantitative immunoblot. Graphical representation of the small IsdC band within the supernatant. Error bars represent average range of biological triplicates. a.u., arbitrary units. * p<.002 (A). Representative IsdC levels as analyzed by immunoblotting. Wildtype *S. lugdunensis* or Δ*pghI* strains were grown in TSB alone or TSB with 350 µM Dip. Arrow indicates IsdC band that is diminished within the Δ*pghI* mutant (B). Graphical representation of IsdC bands within the wall fraction of wildtype and Δ*pghI* mutant. Error bars represent the average range of biological triplicates (C).

PghI is required for biofilm formation

Many of the infections attributed to *S. lugdunensis* are associated with biofilm etiology including native valve endocarditis, intravascular catheter associated infections, and prosthetic joint infections [3]. However, the molecular mechanisms and subsequent regulation that contribute to these biofilms remain poorly understood. Iron restriction is typically encountered within host tissues and consequently many bacterial virulence factors are iron-regulated. Establishing *pghI* as part of the iron-regulated Isd system but lacking a clear definitive role in iron acquisition or cell division lead to the hypothesis that PghI may contribute to biofilm formation in an iron dependent manner. To test this hypothesis wildtype and *ΔpghI* strains were tested for their ability to form biofilms within plasma coated 96 well plates as measured by crystal violet staining. This assay indicated that the level of biofilm formation is reduced within the *ΔpghI* strain and resulted in significantly less crystal violet staining (Figure 13). This change in staining is not due to general growth defects within the mutant strains as biofilm formation was determined by the ratio of crystal violet staining to total growth as measured by O.D. 600. Furthermore, this phenotype was iron dependent such that both the wildtype and the *ΔpghI* mutant created similar biofilms when grown in iron replete media . PghI modulates IsdC release from the cell wall which lead me to hypothesize that this supernatant IsdC facilitates biofilm formation. To test this hypothesis a *ΔisdC S. lugdunensis* strain was tested for its ability to generate biofilms (Figure 13). Similar to the *ΔpghI* mutant the *ΔisdC* strain did not form biofilms at wildtype levels and this phenotype was iron dependent. It remains unclear however if IsdC must be released from the cell wall by PghI to enhance biofilm production therefore additional research needs to be conducted to elucidate whether the IsdC-mediated biofilm formation occurs concomitantly with PghI release of IsdC from the

cell wall or if these two events are unrelated. It is possible that multiple species of IsdC

participate in biofilm matrix production.
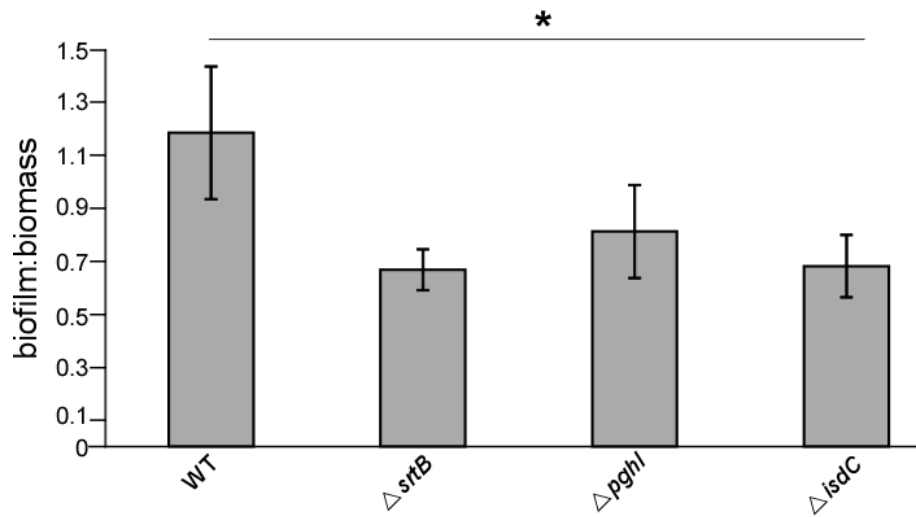
Figure 13. PghI is required for normal biofilm formation.

Biofilm formation relative to total biomass was measured for both wildtype *S. lugdunensis,* a Δ*srtB,* Δ*pghI* and Δ*isdC* strains of *S. lugdunensis.* Error bars represent the average range of biological triplicates. * p<.02.

Discussion

PG hydrolases are a family of enzymes that perform a variety of functions within the bacterial cell. Many hydrolases remodel PG, allowing for cell division and cell wall recycling. Some PG hydrolases induce cell lysis and are referred to as autolysins [17]. Lysing of cells can be beneficial to a species as a whole as it can facilitate biofilm formation through the release of eDNA which promotes adherence to surfaces. Release of eDNA can also promote bacterial survival. For example *Streptococcus pneumonia* releases bacteriolytic PG hydrolases referred to as fratricidins which cause cell lysis of non-competent cells and allow competent cells to acquire the eDNA [76]. This DNA acquisition has been shown to promote survival of the species during periods of stress [76]. Furthermore, the major autolysin within *S. aureus* has been shown to facilitate binding to host factors and subsequently promotes cellular internalization and persistent infections [77]. While there have been a wide range of functions associated with PG hydrolases none have been shown to be iron-regulated or modify the secretion profile of a sortase anchored protein.

Wall anchored proteins allow bacteria to interact with and respond to their environment. Within Gram positive bacteria many of these proteins are covalently linked to the peptidoglycan wall through the enzymatic activity of membrane bound sortases. Proteins destined to be linked to the cell wall by sortases contain signal peptides that are typically located at the C-termini. All Gram-positive bacteria have a sortase A which cleaves the C-terminal LPXTG sorting motif. Within the *S. lugdunensis* Isd system heme binding proteins IsdB and IsdJ possess a sortase A sorting motif and localize to the cell wall. IsdC

and IsdK however have sortase B motifs and while IsdC localizes to the cell wall, the majority of IsdK within the cell is found in the cell membrane [36]. Upon completion of translation precursor proteins (P1) destined for sortase anchoring are exported from the cytoplasm and the NH_2-terminal leader peptide is removed creating the P2 intermediate. P2 is cleaved at the C-terminal sortase motif generating the mature wall anchored protein M. Research I conducted shows that the PghI alters the IsdC secretion profile such that supernatants from wildtype *S. lugdunensis* have two sizes of IsdC while supernatants from the *ΔpghI* strain have significantly less of the larger IsdC species. Importantly, supernatants from a *ΔsrtB* mutant had no detectable IsdC in their supernatant indicating that PghI modulates the M form of IsdC. Interestingly, PghI has a sortase B sorting signal located at the non-canonical N-terminus. While it remains unclear if PghI is a sortase B substrate it is tempting to speculate that PghI is cleaved by sortase B resulting in the co-localization of PghI and IsdC. The specific IsdC modification performed by PghI is currently unknown. One possibility is the PghI protects IsdC from proteolytic cleavage or protects the PG associated peptides to which IsdC is bound from hydrolysis. In the absence of PghI all mature IsdC is processed, resulting in a single smaller species of IsdC. Interestingly, other PG hydrolases with FlgJ domains have been shown to interact with flagellar proteins and protect them from degradation [78]. An additional possibility is that PghI hydrolyzes PG bonds near IsdC resulting in the release of IsdC with PG residues still attached.

The canonical function of IsdC is to transport heme through the PG wall to IsdEF which then transports heme across the membrane. The biological ramifications of releasing IsdC in multiple forms needs to be explored further. It is conceivable that unbound IsdC

could act as a hemophore and bind free extracellular heme and transfer the heme back to the cell. I analyzed the ability of the *ΔpghI* strain to utilize heme or hemoglobin as an iron source and could not detect a growth defect. This does not exclude the possibility of IsdC functioning as a hemophore because iron acquisition phenotypes are incredibly difficult to detect within *S. lugdunensis*.

Biofilms are bacterial communities that adhere to surfaces through extracellular polymeric substances (EPS) [79]. The composition of this EPS varies and can consist of DNA, techoic acids, host plasma factors, and proteinaceous adhesins [79]. Biofilms are clinically significant as they result in refractory infections that are resistant to antibiotics. Indwelling devices can lead to biofilm formation and *S. lugdunensis* has a propensity for causing endocarditis, an infection typically associated with biofilm formation. The role of PG hydrolases in biofilm formation has been well established. Often autolysins will lyse cells, releasing eDNA which then functions as an EPS. My research shows that the PghI facilitates biofilm formation however the role of the PghI in this process has not been elucidated. There is no evidence that PghI promotes cell lysis during exponential growth however it has not been determined if PghI activity accelerates cell lysis during stationary phase therefore it is possible that the enzymatic activity of PghI results in the production of eDNA. Future experiments will focus on investigating if PghI activity mediates autolysis during later growth phases. The PghI-mediated release of IsdC may facilitate bacterial adhesion and subsequent biofilm formation. In support of this, I found that a *ΔisdC* mutant strain of *S. lugdunensis* has reduced biofilm formation comparable to that of the *ΔpghI* strain. It remains unclear how IsdC facilitates biofilm production or which IsdC species is involved in biofilm formation. It is tempting to speculate that IsdC, upon being released

from the cell wall by PghI, mediates bacterial adherence and biofilm establishment. It is possible however that PghI is involved in biofilm formation in an IsdC independent manner. When supernatants from both the wildtype and Δ*pghI* strain were analyzed by silver stain IsdC was the only protein that differed between the two strains. It is possible that PghI modifies additional proteins that enhance bacterial adhesion but were not detectable by silver stain. Additionally, PghI may promote adhesion directly as the major autolysin, Atl, does within *S. aureus*. The propensity of *S. lugdunensis* to cause infections typically associated with biofilm production underscores the necessity to identify proteins involved in this process. Further research on PghI activity could provide vital insight into the pathogenesis of *S. lugdunensis.*

Chapter IV

CONCLUSIONS

Summary

Most bacterial pathogens require iron for growth including *S. lugdunensis* (Figure 2A). The vertebrate host exploits this iron requirement by deploying numerous iron binding proteins including lactoferrin, transferrin and ferritin which rapidly remove all free iron [31]. Additionally, the majority of iron in the human body is found in the form of heme which is bound by hemoproteins, the most abundant of which is hemoglobin. To further sequester iron, hemoglobin is stored within erythrocytes. To gain access to the iron within hemoglobin bacterial pathogens utilize an arsenal of virulence factors. *S. lugdunensis* expresses a delta hemolysin which lysis red blood cells and provides *S. lugdunensis* physical access to host hemoglobin [14]. This liberated hemoglobin is then bound via proteins within the Isd system which remove heme from hemoglobin, transport the heme across the cell wall and membrane and upon entering the cytoplasm the heme is degraded to release iron (Figure 14). This heme catabolism is performed by a cytoplasmic IsdG-family heme oxygenase (Chapter II).

Although *S. lugdunensis* encodes within its genome a complete Isd system the enzymatic activity had not been characterized for any of the *S. lugdunensis* Isd proteins. Sequence analysis revealed the presence of Fur boxes upstream of the IsdC, IsdJ and IsdB start sites however iron-regulated transcription had not been confirmed for this locus. My work has demonstrated that the *S. lugdunensis* Isd system is up-regulated upon iron starvation which results in the increased abundance of cytoplasmic IsdG (Chapter II and

III). I have also established that *S. lugdunensis* IsdG is capable of binding and catabolizing heme. Furthermore, I have shown that *S. lugdunensis* IsdG expressed *in trans* within a *S. aureus ΔisdGΔisdI* mutant is able to complement the heme utilization defect of this strain indicating that *S. lugdunensis* IsdG-mediated heme degradation enables the use of heme as a nutrient iron source (Chapter II).

The Isd system within *S. aureus* encodes two heme oxygenases, IsdG and IsdI, which are differentially regulated by iron and heme. Both *isdG* and *isdI* transcription levels increase in iron deplete conditions, however IsdG is proteolytically degraded in the absence of heme while IsdI is constitutively stable [34]. At the amino acid level *S. lugdunensis* IsdG is 68% identical to *S. aureus* IsdG yet I have shown that *S. lugdunensis* IsdG is regulated in a manner similar to *S. aureus* IsdI and is stable independent of heme binding (Chapter II). This data suggests that *S. lugdunensis* does not regulate heme catabolism as tightly as *S. aureus.* Differences in heme oxygenase regulation between *S. aureus* and *S. lugdunensis* may be due to variances in the rate of exogenous heme influx or endogenous heme synthesis.

Heme oxygenases are a ubiquitous family of enzymes which degrade the tetrapyrole heme to release free iron and are conserved within vertebrates, plants and bacteria. Heme oxygenases are divided into two families, the HO-1 family of heme oxygenases and the IsdG-family of heme oxygenases. The catabolism of heme by HO-1 heme oxygenases results in the production of α-biliverdin and carbon monoxide [59]. The IsdG-family of heme oxygenases in contrast degrade heme to the chromophore staphylobilin and formaldehyde [68] with the exception of the *M. tuberculosis* IsdG which degrades heme to mycobilin. The role of HO-1 mediated heme degradation products has been well

established but the biological ramifications of staphylobilin production have not yet been determined. Our work demonstrates that *S. lugdunensis* IsdG also degrades heme to staphylobilin thus establishing staphylobilin as the conserved degradation product of the IsdG-family of heme oxygenases within *Staphylococci*. Moreover, analysis of all sequenced bacterial genomes revealed the presence of predicted IsdG orthologs within a diverse range of bacterial species. This finding indicates the use of IsdG for heme degradation and subsequent regulation is a common strategy among bacteria and suggests a possible universal role for staphylobilin production in bacteria (Chapter II).

In Chapter III I describe the elucidation of a PG hydrolase within the *S. lugdunensis* Isd operon. My work establishes the inclusion of *pghI* within the *S. lugdunensis* Isd operon and confirms that *pghI* is transcriptionally up-regulated along with the entire Isd locus during periods of iron starvation. Prior to my work *pghI* was predicted to encode for a PG hydrolase however no biochemical research had been conducted to confirm the enzymatic function of PghI. My research confirms that recombinant PghI is capable of hydrolyzing PG. Importantly, these results are the first to establish the inclusion of a PG hydrolase within an Isd system. The biological relevance of coordinating expression of a PG hydrolase along with heme-iron acquisition proteins is an area of active research. Many of the Isd proteins are anchored to the PG cell wall and localize to the bacterial surface where they interact with the extracellular environment. The biological pathways that target proteins for secretion and PG linkage are well studied yet how these proteins, which are often large, traverse through the rigid PG wall remains unknown. One possible rationale for including *pghI* within the Isd operon could be to facilitate PG rearrangement that allows Isd wall anchored proteins to localize on the outside of the cell. IsdC is

predicted to be embedded throughout the cell wall thus creating a channel which heme can pass through. Additionally, it is conceivable that PghI ensures that IsdC is evenly and consistently placed throughout the cell wall.

Biofilms are complex communities of bacteria which are of particular clinical significance due to their increased resistance to antibiotics and association with refractory infections. The formation of biofilms is a complex and dynamic process that frequently is associated with PG hydrolase activity. My research demonstrates that *S. lugdunensis* produces a biofilm within an iron limiting environment and that formation of this biofilm requires PghI activity. How *S. lugdunensis* adheres to surfaces and forms an extracellular matrix to establish a biofilm remains unknown however research I have conducted has identified potential molecular mechanisms utilized by *S. lugdunensis* during biofilm formation. My work shows that PghI modulates mature IsdC release from the staphylococcal cell wall (Figures 12 and 14). Many bacteria create biofilms through protein secretion and therefore it is plausible that released IsdC is a constituent of the extracellular matrix and that PghI mediated release of IsdC enhances matrix formation. Future research will focus on identifying the specific molecular constituents within *S. lugdunensis* biofilm matrixes and more precisely defining the roles of PghI and IsdC in the formation of the matrix.
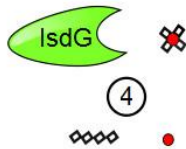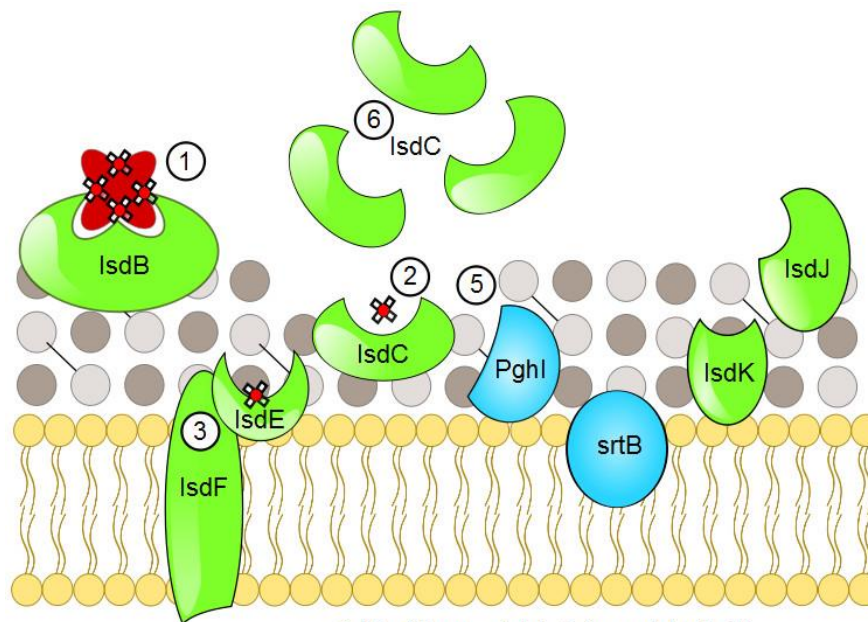
1. Host hemoglobin is bound by IsdB.
2. Heme is extracted from hemoglobin and is transferred to IsdC.
3. Heme is transferred from IsdC to IsdEF which allows the passage of heme through the cell membrane.
4. Cytoplasmic heme is degraded by IsdG to release free iron and produce staphylobilin.
5. PghI hydrolyzes PG within the cell wall.
6. PghI modulates the release of IsdC from the cell wall.

Figure 14.

Model illustrating the role of IsdG and PghI within the *S. lugdunensis* Isd system.

Future Directions

Identify the residues required for PghI enzymatic activity

Comparative studies of the primary structure of PghI with proteins with known PG hydrolyzing activity suggest that the N-terminus of PghI contains an FlgJ domain including conserved residues, aspartic acid and glutamic acid. These conserved residues are located in the active center of multiple muramidases. The C-terminus of PghI has a predicted cysteine, histidine dependent amidohydrolase/peptidase (CHAP) domain. Previous research has shown that CHAP domains have two invariant residues, cysteine and histidine, both of which are conserved within PghI [80]. These conserved residues will be targeted for mutagenesis. The generation of point mutants will be done using a pfu mutagenesis technique. Mutant forms of PghI will be created in both an over-expression vector to allow for recombinant protein purification as well as a constitutive expression vector for complementation studies. We will purify mutant forms of recombinant PghI using our established protocol. Proteins will be assessed for proper expression by SDS-PAGE and proper folding will be determined using circular dichroism spectroscopy at the Structural Biology Core Facility located at Vanderbilt University. Purified mutant PghI will be analyzed for enzymatic activity using a zymogram assay. Additionally, mutant PghI activity will be analyzed through complementation assays in which mutant *pghI* is expressed within *ΔpghI S. lugdunensis* cells and supernatants assessed to determine if mutant PghI can complement the IsdC release defect. Biofilm formation will also be measured within *ΔpghI* strains complemented with mutant forms of *pghI* and allow us to determine if the PG hydrolyzing activity of PghI is required for biofilm establishment. Together, these experiments will allow us to define the amino acid residues required for the enzymatic activity of PghI as well as confirm the designation of an FlgJ and CHAP

domain within PghI. Furthermore, we will determine if modulation of IsdC release and biofilm formation are dependent upon the ability of PghI to hydrolyze PG.

Determine if PghI is a sortase B substrate

Analysis of the primary sequence of PghI revealed a putative sortase B sorting motif. Sortase sorting signals are typically located at the C-terminus upstream of a stretch of hydrophobic residues however; the sortase B signal in PghI is located at the N-terminus between a disordered domain and the FlgJ domain. To determine if PghI is a sortase B substrate, we will create a myc-tagged version of PghI which is expressed from a constitutive expression vector. Expression vectors will be created to add a myc-tag to both the N and C termini. These vectors will be transformed into both wildtype *S. lugdunensis* as well as a *ΔsrtB* mutant strain and the localization of PghI will be assessed by first fractionating cells and then analyzing each fraction by western-blot analysis using myc specific antibodies. If PghI is indeed a sortase B substrate, we should be able to detect PghI within the wall fraction of wildtype cells and within the membrane fraction of the *ΔsrtB* mutant.

If it is determined that PghI is a sortase B substrate, expression vectors will be constructed in which point mutations within the NPQTS sorting motif have been created to ablate sortase B cleavage and subsequent linkage of PghI to the PG wall. Expression of this vector in a *ΔpghI* mutant will allow us to elucidate what contribution sortase B anchoring has on PghI activity. Furthermore, we will probe the supernatants for IsdC using western blot analysis to determine if sortase B processing is required for PghI-mediated release of IsdC from the cell wall. Additionally, biofilm production will be

measured in this strain to define if sortase B cleavage of PghI is necessary for PghI dependent biofilm formation.

Elucidate the specific modification of IsdC mediated by PghI

I have demonstrated that after IsdC is covalently anchored to the cell wall PghI facilitates the release of IsdC into the extracellular milieu. How specifically PghI modulates the release of IsdC is not known. To determine how IsdC has been modified by PghI we will perform pull-down assays in which IsdC will be removed from the supernatant of wildtype and Δ*pghI* mutant cultures using IsdC specific antibodies. Protein-A sepharose beads will be used to remove anti-IsdC antibodies and associated proteins. Proteins that co-precipitate with the IsdC antibodies will then be separated by SDS-PAGE. The SDS-PAGE will then be stained with colloidal blue and bands corresponding to the sizes of both species of IsdC will be removed and analyzed by Multi-Dimmensional Protein Identification Technology (MuDPIT) at the Mass Spectrometry Research Lab at Vanderbilt University. This analysis will enable us to identify differences between both IsdC sizes at the amino acid level. Additionally, if IsdC is still bound to PG fragments these fragments can be detected using MuDPIT. Together, these experiments will elucidate the specific PghI-mediated modifications of of IsdC and determine if either IsdC species is still bound to PG moieties.

Identify how PghI promotes biofilm formation

Bacterial biofilms require the production of an extracellular polymeric matrix. This matrix is predominantly self-produced and can be composed of proteins, eDNA, techoic acids and polysaccharides. My research demonstrates that *S. lugdunensis* generates a

biofilm during iron starvation and that PghI and IsdC are required for this biofilm formation. The mechanism by which PghI contributes to this bacterial community remains undefined however, it is possible that IsdC released from the cell by PghI activity aids bacterial adherence or is a matrix constituent and therefore the biofilm phenotypes of both the *ΔpghI* and *ΔisdC* strains are linked. To test this hypothesis biofilm production of the *ΔpghI* strain grown in media supplemented with supernatants collected from wildtype cultures will be measured. If IsdC released from the cells by PghI is responsible for the *ΔpghI* biofilm phenotype then wildtype supernatants containing this IsdC species should complement the biofilm defect. To confirm that it is specifically IsdC in wildtype cultures that complements the *ΔpghI* phenotype supernatants from *ΔisdC* cultures will also be tested.

Many PG hydrolases promote biofilm formation through cell lysis and subsequent eDNA release. While no growth phenotype has been found in the *ΔpghI* mutant during early exponential through early stationary growth phases it is conceivable that PghI activity induces cell lysis during stationary phase. In fact, the major autolysin within *S. aureus*, Atl, does not contribute to cell lysis until cells have reached stationary phase [81]. To elucidate if PghI activity stimulates cell lysis the OD_{600} of wildtype and *ΔpghI* cells will be monitored throughout all growth phases including stationary phase. The OD_{600} measurement in stationary phase of wildtype cells will decrease as cells lyse, however if PghI promotes autolysis the OD_{600} value will remain relatively constant. Furthermore, this assay will be done on cells grown in both iron replete and iron deplete media to ensure that any phenotype observed within the *ΔpghI* strain is iron dependent. Additionally, eDNA production of wildtype and *ΔpghI* cells can be measured directly by culturing the

strains in media supplemented with propidium iodide which fluoresces when bound to DNA but does not penetrate live bacteria. The eDNA can therefore be measured using a microtitre plate reader. Together these experiments will deduce whether PghI expression promotes cell lysis and subsequent eDNA release.

In addition to promoting biofilm formation through the production of eDNA many PG hydrolases aid biofilm formation by promoting bacterial adhesion. To determine if PghI participates in the initial binding to foreign surfaces a primary attachment assay will be conducted in which the ability of both wildtype and *ΔpghI* cells to adhere to polysterene that has been coated with plasma will be measured. In this assay overnight cultures are normalized to the same total colony forming units (CFU) and then briefly applied to treated polysterene petri dishes. Unattached cells are then removed using multiple PBS washes. Next molten agar is poured onto the plates and the plates are then incubated to allow bacterial growth. Primary attachment is expressed as the percent of original CFUs which remain attached as indicated by colony formation. If PghI promotes biofilm production by assisting in the initial attachment of bacteria then a greater percentage of the *ΔpghI* cells will be washed off the plates resulting in decreased CFUs. Additionally, by treating cells with DNAse prior to plating this assay can be utilized to determine if PghI facilitates initial attachment through eDNA production.

Determine if PghI facilitates extracellular protein localization

The inclusion of a PG hydrolase is unique to the *S. lugdunensis* Isd system, however a role in iron acquisition has not been identified for PghI. One possible explanation for co-transcribing *pghI* with the rest of the Isd system is that PghI-mediated PG hydrolysis

enables proper placement of wall anchored proteins, specifically IsdC which is predicted to be embedded continuously throughout all layers of the PG wall. To test this hypothesis localization of IsdC on the bacterial surface of wildtype and *ΔpghI* cells could be analyzed using immunofluorescence. If PghI promotes proper placement and movement of IsdC through the PG layers less IsdC should be present on the surface of the *ΔpghI* cells. Additionally, PghI may expedite the process of IsdC localization within the wall resulting in slower appearance of IsdC on the surface of *ΔpghI* cells. To test this model, all extracellular proteins would be removed from the cell wall through proteinase K treatment and cells subsequently measured for surface levels of IsdC at various time points using immunofluorescence. If PghI accelerates the placement of IsdC through the PG wall then reappearance of extracellular IsdC should occur more rapidly in wildtype cells than in *ΔpghI* cells. Together these experiments would elucidate if PghI facilitates IsdC movement and localization within the PG wall. Furthermore, these experiments could be extrapolated to examine the influence of PghI on the localization of additional wall anchored proteins including IsdB, IsdK and IsdJ.

LIST OF PUBLICATIONS

Pischany, G., Haley, K.P., Skaar, E.P., *Staphylococcus aureus* growth using human hemoglobin as an iron source. 2013. *J. Vis. Exp.* (72), e50072, doi:10.3791/50072

Haley, K. P., Skaar, E. P., A battle for iron: host sequestration and *Staphylococcus aureus* acquisition. 2011. *Microbes Infect.* 14(3):217-27

Haley, K. P., Janson, E. M., Heilbronner, S., Foster, T. J., Skaar, E. P., *Staphylococcus lugdunensis* IsdG liberates iron from host heme. 2011. *J. Bacteriol.* 193:18 4743-4757

Reniere, M. L., Haley, K. P., Skaar, E. P., The flexible loop of *Staphylococcus aureus* IsdG is required for its degradation in the absence of heme. 2011. *Biochemistry*. 50 (31), 6730-6737

Jiang, W., Lederman, M.M., Hunt, P., Sieg, S.F., Haley, K. P., Rodriguez, B., Landay, A., Martin, J., Sinclair, E., Asher, A. I., Deeks, S. G., Douek, D. C., Brenchley, J.M., Plasma levels of bacterial DNA correlate with immune activation and the magnitude of immune restoration in persons with antiretroviral-treated HIV infection. 2009. *J. Infect. Disease*. 199 (8): 1177-1185.

BIBLIOGRAPHY

1.   Sotutu, V., et al., *The "surreptitious Staphylococcus": Staphylococcus lugdunensis endocarditis in a child.* Pediatr Infect Dis J, 2002. **21**(10): p. 984-6.

2.   Frank, K.L., J.L. Del Pozo, and R. Patel, *From clinical microbiology to infection pathogenesis: how daring to be different works for Staphylococcus lugdunensis.* Clin Microbiol Rev, 2008. **21**(1): p. 111-33.

3.   Arias, M., et al., *Skin and soft tissue infections caused by Staphylococcus lugdunensis: report of 20 cases.* Scand J Infect Dis, 2010. **42**(11-12): p. 879-84.

4.   Hung, T., et al., *Necrotizing Fasciitis Associated with Staphylococcus lugdunensis.* Case Rep Infect Dis, 2012. **2012**: p. 453685.

5.   Anguera, I., et al., *Staphylococcus lugdunensis infective endocarditis: description of 10 cases and analysis of native valve, prosthetic valve, and pacemaker lead endocarditis clinical profiles.* Heart, 2005. **91**(2): p. e10.

6.   Kleiner, E., et al., *Clinical significance of Staphylococcus lugdunensis isolated from routine cultures.* Clin Infect Dis, 2010. **51**(7): p. 801-3.

7.   Vandenesch, F., et al., *Endocarditis due to Staphylococcus lugdunensis: report of 11 cases and review.* Clin Infect Dis, 1993. **17**(5): p. 871-6.

8.   Tee, W.S., et al., *Staphylococcus lugdunensis carrying the mecA gene causes catheter-associated bloodstream infection in premature neonate.* J Clin Microbiol, 2003. **41**(1): p. 519-20.

9.   Frank, K.L., et al., *In vitro effects of antimicrobial agents on planktonic and biofilm forms of Staphylococcus lugdunensis clinical isolates.* Antimicrob Agents Chemother, 2007. **51**(3): p. 888-95.

10.   Vandenesch, F., et al., *Agr-related sequences in Staphylococcus lugdunensis.* FEMS Microbiol Lett, 1993. **111**(1): p. 115-22.

11.   Nilsson, M., et al., *A fibrinogen-binding protein of Staphylococcus lugdunensis.* FEMS Microbiol Lett, 2004. **241**(1): p. 87-93.

12.   Moreillon, P., et al., *Role of Staphylococcus aureus coagulase and clumping factor in pathogenesis of experimental endocarditis.* Infect Immun, 1995. **63**(12): p. 4738-43.

13.   McAdow, M., D.M. Missiakas, and O. Schneewind, *Staphylococcus aureus secretes coagulase and von Willebrand factor binding protein to modify the coagulation cascade and establish host infections.* J Innate Immun, 2012. **4**(2): p. 141-8.

14.   Vandenesch, F., et al., *Delta-like haemolysin produced by Staphylococcus lugdunensis.* FEMS Microbiol Lett, 1991. **62**(1): p. 65-8.

15.   Uehara, T. and T.G. Bernhardt, *More than just lysins: peptidoglycan hydrolases tailor the cell wall.* Curr Opin Microbiol, 2011. **14**(6): p. 698-703.

16.   Johnson, J.W., J.F. Fisher, and S. Mobashery, *Bacterial cell-wall recycling.* Ann N Y Acad Sci, 2013. **1277**: p. 54-75.

17.   Vollmer, W., et al., *Bacterial peptidoglycan (murein) hydrolases.* FEMS Microbiol Rev, 2008. **32**(2): p. 259-86.

18.   Dufour, D. and C.M. Levesque, *Cell death of Streptococcus mutans induced by a quorum-sensing peptide occurs via a conserved streptococcal autolysin.* J Bacteriol, 2013. **195**(1): p. 105-14.

19.   Humann, J., et al., *Expression of the p60 autolysin enhances NK cell activation and is required for listeria monocytogenes expansion in IFN-gamma-responsive mice.* J Immunol, 2007. **178**(4): p. 2407-14.

20.   Ramos-Sevillano, E., et al., *Nasopharyngeal colonization and invasive disease are enhanced by the cell wall hydrolases LytB and LytC of Streptococcus pneumoniae.* PLoS One, 2011. **6**(8): p. e23626.

21.   Fitzpatrick, F., H. Humphreys, and J.P. O'Gara, *The genetics of staphylococcal biofilm formation--will a greater understanding of pathogenesis lead to better*

management of device-related infection? Clin Microbiol Infect, 2005. **11**(12): p. 967-73.

22. Montanaro, L., et al., *Extracellular DNA in biofilms.* Int J Artif Organs, 2011. **34**(9): p. 824-31.

23. Heilmann, C., et al., *Evidence for autolysin-mediated primary attachment of Staphylococcus epidermidis to a polystyrene surface.* Mol Microbiol, 1997. **24**(5): p. 1013-24.

24. Bullen, J.J., et al., *Iron and infection: the heart of the matter.* FEMS Immunol Med Microbiol, 2005. **43**(3): p. 325-30.

25. Wessling-Resnick, M., *Iron homeostasis and the inflammatory response.* Annu Rev Nutr, 2010. **30**: p. 105-22.

26. Drabkin, D.L., *Metabolism of the hemin chromoproteins.* Physiol Rev, 1951. **31**(4): p. 345-431.

27. Oliviero, S., G. Morrone, and R. Cortese, *The human haptoglobin gene: transcriptional regulation during development and acute phase induction.* EMBO J, 1987. **6**(7): p. 1905-12.

28. Dryla, A., et al., *Identification of a novel iron regulated staphylococcal surface protein with haptoglobin-haemoglobin binding activity.* Mol Microbiol, 2003. **49**(1): p. 37-53.

29. Torres, V.J., et al., *Staphylococcus aureus IsdB is a hemoglobin receptor required for heme iron utilization.* J Bacteriol, 2006. **188**(24): p. 8421-9.

30. Fowler, V.G., Jr., et al., *Staphylococcus aureus endocarditis: a consequence of medical progress.* JAMA, 2005. **293**(24): p. 3012-21.

31. Ganz, T., *Hepcidin and iron regulation, 10 years later.* Blood, 2011. **117**(17): p. 4425-33.

32. Reniere, M.L., et al., *The IsdG-family of haem oxygenases degrades haem to a novel chromophore.* Mol Microbiol, 2010. **75**(6): p. 1529-38.

33. Nambu, S., et al., *A new way to degrade heme: the Mycobacterium tuberculosis enzyme MhuD catalyzes heme degradation without generating CO.* J Biol Chem, 2013. **288**(14): p. 10101-9.

34. Reniere, M.L. and E.P. Skaar, *Staphylococcus aureus haem oxygenases are differentially regulated by iron and haem.* Mol Microbiol, 2008. **69**(5): p. 1304-15.

35. Skaar, E.P., A.H. Gaspar, and O. Schneewind, *IsdG and IsdI, heme-degrading enzymes in the cytoplasm of Staphylococcus aureus.* J Biol Chem, 2004. **279**(1): p. 436-43.

36. Zapotoczna, M., et al., *Iron-regulated surface determinant (Isd) proteins of Staphylococcus lugdunensis.* J Bacteriol, 2012. **194**(23): p. 6453-67.

37. Haley, K.P., et al., *Staphylococcus lugdunensis IsdG liberates iron from host heme.* J Bacteriol, 2011.

38. Grigg, J.C., et al., *Structural biology of heme binding in the Staphylococcus aureus Isd system.* J Inorg Biochem, 2010. **104**(3): p. 341-8.

39. Mazmanian, S.K., et al., *Staphylococcus aureus sortase mutants defective in the display of surface proteins and in the pathogenesis of animal infections.* Proc Natl Acad Sci U S A, 2000. **97**(10): p. 5510-5.

40. Pilpa, R.M., et al., *Solution structure of the NEAT (NEAr Transporter) domain from IsdH/HarA: the human hemoglobin receptor in Staphylococcus aureus.* J Mol Biol, 2006. **360**(2): p. 435-47.

41. Grigg, J.C., et al., *Haem recognition by a Staphylococcus aureus NEAT domain.* Mol Microbiol, 2007. **63**(1): p. 139-49.

42. Lindsay, J.A. and T.V. Riley, *Staphylococcal iron requirements, siderophore production, and iron-regulated protein expression.* Infect Immun, 1994. **62**(6): p. 2309-14.

43. Friedman, D.B., et al., *Staphylococcus aureus redirects central metabolism to increase iron availability.* PLoS Pathog, 2006. **2**(8): p. e87.

44.   Beasley, F.C. and D.E. Heinrichs, *Siderophore-mediated iron acquisition in the staphylococci.* J Inorg Biochem, 2010. **104**(3): p. 282-8.

45.   Skaar, E.P., et al., *Iron-source preference of Staphylococcus aureus infections.* Science, 2004. **305**(5690): p. 1626-8.

46.   Braun, V., K. Gunter, and K. Hantke, *Transport of iron across the outer membrane.* Biol Met, 1991. **4**(1): p. 14-22.

47.   Skaar, E.P., A.H. Gaspar, and O. Schneewind, *Bacillus anthracis IsdG, a heme-degrading monooxygenase.* J Bacteriol, 2006. **188**(3): p. 1071-80.

48.   Tse, H., et al., *Complete genome sequence of Staphylococcus lugdunensis strain HKU09-01.* J Bacteriol, 2010. **192**(5): p. 1471-2.

49.   E. S. Duthie, L.L., Lorenz, *Staphylococcal Coagulase: Mode of Action and Antigenicity.* Journal of General Microbiology, 1952. **6**: p. 95-107.

50.   Bubeck Wardenburg, J., W.A. Williams, and D. Missiakas, *Host defenses against Staphylococcus aureus infection require recognition of bacterial lipoproteins.* Proc Natl Acad Sci U S A, 2006. **103**(37): p. 13831-6.

51.   Schneewind, O., P. Model, and V.A. Fischetti, *Sorting of protein A to the staphylococcal cell wall.* Cell, 1992. **70**(2): p. 267-81.

52.   Edgar, R.C., *MUSCLE: multiple sequence alignment with high accuracy and high throughput.* Nucleic Acids Res, 2004. **32**(5): p. 1792-7.

53.   Kumar, S. and M. Nei, *Molecular evolution and phylogenetics*, in *Oxford University Press, New York.*2000.

54.   Abascal, F., R. Zardoya, and D. Posada, *ProtTest: selection of best-fit models of protein evolution.* Bioinformatics, 2005. **21**(9): p. 2104-5.

55.   Whelan, S. and N. Goldman, *A general empirical model of protein evolution derived from multiple protein families using a maximum-likelihood approach.* Mol Biol Evol, 2001. **18**(5): p. 691-9.

56. Guindon, S. and O. Gascuel, *A simple, fast, and accurate algorithm to estimate large phylogenies by maximum likelihood.* Syst Biol, 2003. **52**(5): p. 696-704.

57. Guindon, S., et al., *New algorithms and methods to estimate maximum-likelihood phylogenies: assessing the performance of PhyML 3.0.* Syst Biol, 2010. **59**(3): p. 307-21.

58. Wu, R., et al., *Staphylococcus aureus IsdG and IsdI, heme-degrading enzymes with structural similarity to monooxygenases.* J Biol Chem, 2005. **280**(4): p. 2840-6.

59. Unno, M., et al., *Crystal structure of the dioxygen-bound heme oxygenase from Corynebacterium diphtheriae: implications for heme oxygenase function.* J Biol Chem, 2004. **279**(20): p. 21055-61.

60. Noguchi, M., T. Yoshida, and G. Kikuchi, *Purification and properties of biliverdin reductases from pig spleen and rat liver.* J Biochem, 1979. **86**(4): p. 833-48.

61. Chipperfield, J.R. and C. Ratledge, *Salicylic acid is not a bacterial siderophore: a theoretical study.* Biometals, 2000. **13**(2): p. 165-8.

62. Chim, N., et al., *Unusual diheme conformation of the heme-degrading protein from Mycobacterium tuberculosis.* J Mol Biol, 2010. **395**(3): p. 595-608.

63. Puri, S. and M.R. O'Brian, *The hmuQ and hmuD genes from Bradyrhizobium japonicum encode heme-degrading enzymes.* J Bacteriol, 2006. **188**(18): p. 6476-82.

64. Mazmanian, S.K., et al., *Passage of heme-iron across the envelope of Staphylococcus aureus.* Science, 2003. **299**(5608): p. 906-9.

65. Skaar, E.P. and O. Schneewind, *Iron-regulated surface determinants (Isd) of Staphylococcus aureus: stealing iron from heme.* Microbes Infect, 2004. **6**(4): p. 390-7.

66. Kirkby, K.A. and C.A. Adin, *Products of heme oxygenase and their potential therapeutic applications.* Am J Physiol Renal Physiol, 2006. **290**(3): p. F563-71.

67. Stocker, R., et al., *Bilirubin is an antioxidant of possible physiological importance.* Science, 1987. **235**(4792): p. 1043-6.

68. Matsui, T., et al., *Heme degradation by Staphylococcus aureus IsdG and IsdI liberates formaldehyde rather than carbon monoxide.* Biochemistry, 2013. **52**(18): p. 3025-7.

69. Josefsson, E., et al., *Protection against experimental Staphylococcus aureus arthritis by vaccination with clumping factor A, a novel virulence determinant.* J Infect Dis, 2001. **184**(12): p. 1572-80.

70. Berry, A.M., et al., *Contribution of autolysin to virulence of Streptococcus pneumoniae.* Infect Immun, 1989. **57**(8): p. 2324-30.

71. Berry, A.M. and J.C. Paton, *Additive attenuation of virulence of Streptococcus pneumoniae by mutation of the genes encoding pneumolysin and other putative pneumococcal virulence proteins.* Infect Immun, 2000. **68**(1): p. 133-40.

72. Rupp, M.E., et al., *Characterization of the importance of polysaccharide intercellular adhesin/hemagglutinin of Staphylococcus epidermidis in the pathogenesis of biomaterial-based infection in a mouse foreign body infection model.* Infect Immun, 1999. **67**(5): p. 2627-32.

73. Lenz, L.L., et al., *SecA2-dependent secretion of autolytic enzymes promotes Listeria monocytogenes pathogenesis.* Proc Natl Acad Sci U S A, 2003. **100**(21): p. 12432-7.

74. Mazmanian, S.K., et al., *An iron-regulated sortase anchors a class of surface protein during Staphylococcus aureus pathogenesis.* Proc Natl Acad Sci U S A, 2002. **99**(4): p. 2293-8.

75. Maresso, A.W., T.J. Chapa, and O. Schneewind, *Surface protein IsdC and Sortase B are required for heme-iron scavenging of Bacillus anthracis.* J Bacteriol, 2006. **188**(23): p. 8145-52.

76. Wei, H. and L.S. Havarstein, *Fratricide is essential for efficient gene transfer between pneumococci in biofilms.* Appl Environ Microbiol, 2012. **78**(16): p. 5897-905.

77.   Hirschhausen, N., et al., *A novel staphylococcal internalization mechanism involves the major autolysin Atl and heat shock cognate protein Hsc70 as host cell receptor.* Cell Microbiol, 2010. **12**(12): p. 1746-64.

78.   de la Mora, J., et al., *The C terminus of the flagellar muramidase SltF modulates the interaction with FlgJ in Rhodobacter sphaeroides.* J Bacteriol, 2012. **194**(17): p. 4513-20.

79.   Brooks, J.L. and K.K. Jefferson, *Staphylococcal biofilms: quest for the magic bullet.* Adv Appl Microbiol, 2012. **81**: p. 63-87.

80.   Zou, Y. and C. Hou, *Systematic analysis of an amidase domain CHAP in 12 Staphylococcus aureus genomes and 44 staphylococcal phage genomes.* Comput Biol Chem, 2010. **34**(4): p. 251-7.

81.   Bose, J.L., et al., *Contribution of the Staphylococcus aureus Atl AM and GL murein hydrolase activities in cell division, autolysis, and biofilm formation.* PLoS One, 2012. **7**(7): p. e42244.